Supplementation of Dimethylglycine Sodium Salt Improves Growth Performance and Intestinal Barrier Function in Piglets With Intrauterine Growth Restriction During the Suckling Period

Kaiwen Bai
Nanjing Agricultural University - Weigang Campus: Nanjing Agricultural University
Luyi Jiang
Zhejiang University - Zijingang Campus: Zhejiang University
Qiming Li
Nanjing Agricultural University - Weigang Campus: Nanjing Agricultural University
Jingfei Zhang
Nanjing Agricultural University - Weigang Campus: Nanjing Agricultural University
Lili Zhang
Nanjing Agricultural University - Weigang Campus: Nanjing Agricultural University
Tian Wang (tianwangnjau@163.com)
Nanjing Agricultural University https://orcid.org/0000-0002-9038-5009

Research

Keywords: Intrauterine growth restriction, newborn piglet, small intestine, redox status, mitochondrial function, dimethylglycine sodium salt

Posted Date: July 20th, 2021

DOI: https://doi.org/10.21203/rs.3.rs-699318/v1

Abstract

Background: Few studies are available on intestinal barrier function in newborn piglets with intrauterine growth restriction (IUGR). Therefore, this study aimed to investigate the mechanism of intestinal dysfunction in IUGR suckling piglets and improve their growth performance using dimethylglycine sodium salt (DMG-Na) supplementation.

Results: The body weights of piglets in the I and ID groups were similar, and both were lower than those in the N and ND groups. However, after 17 days of age, the ID group showed larger ($P < 0.05$) increases in body weight than did the I group. The hub genes were identified from the data analyzed using RNA-seq and WGCNA. Among these, ATP8 was the most significantly changed, and this gene is crucial in maintaining mitochondrial function. The small intestinal histological morphology, redox status, mitochondrial redox status, oxidative damage, and gene and protein expression levels were worse in the IUGR group than in the NBW group. An increasing trend of the small intestinal histological morphology, redox status, mitochondrial redox status, oxidative damage, and gene and protein expression levels was found between the newborn piglets of the NBW and IUGR groups and the day 21 piglets of the N and I groups, respectively. In addition, supplementation of DMG-Na (ND and ID groups) improved the small intestinal histological morphology, redox status, mitochondrial redox status, oxidative damage, and gene and protein expression levels relative to the non-supplemented groups (N and I groups).

Conclusions: The activity of SIRT1/PGC1α was inhibited in IUGR newborn piglets, which led to damage to their intestinal redox status and structure and barrier functions, and lowered their performance. Supplementation with antioxidant substances such as DMG-Na activated SIRT1/PGC1α in IUGR piglets, thereby improving their body state.

Background

Intrauterine growth restriction (IUGR), a condition resulting in fetuses with weight below either the 10th - centile or the population mean minus 2 standard deviations of a population-based nomogram, is an important problem in animal husbandry [1, 2]. IUGR has a permanent stunting effect on postnatal growth and the nutrient utilization efficiency in offspring, and thus impairs long-term health [3, 4]. The gastrointestinal tract is crucial for digestion, absorption, and metabolism of dietary nutrients. However, little is known about the postnatal effects of IUGR on the structure and function of the small intestine during the suckling period. The small intestine is involved in the first steps of postnatal immune system maturation; body protection against food allergens and environmental microorganisms, and nutrient assimilation. After birth, altered gastrointestinal function may lead to diseases, and slow gastrointestinal growth during the suckling period may therefore contribute to slow postnatal growth in neonates with IUGR. Likewise, altered redox status of the gastrointestinal tract may compromise the health of neonates with IUGR throughout the postnatal stage and later on into adulthood [5]. Oxidative damage caused by an imbalance between the antioxidant system and free radical generation system leads to an increase in reactive oxygen species (ROS), which mediate mitochondrial and tissue damage. Mitochondria convert

nutrients into energy through cellular respiration and are the principal energy sources of cells. Compromised mitochondrial function has been linked to numerous diseases, including IUGR [6, 7].

Dimethylglycine sodium salt (DMG-Na) can improve body immunity and relieve oxidative damage by scavenging excess free radicals [8]. DMG-Na is similar to choline and betaine and can improve redox status by acting as an important material for the synthesis of glutathione [9]. Previous studies have found that DMG-Na can relieve oxidative damage and improve offspring performance [9]. DMG-Na not only improves the utilization of oxygen to protect the body from excess free radicals, but also enhances the immune response of individuals [10, 11]. In this study, the ATP8 gene, analyzed by RNA-seq and weighted gene co-expression network analysis (WGCNA), was found to be important in maintaining mitochondrial function. Meanwhile, decreased SIRT1 activity could damage the redox status and suppress the mitochondrial function of the jejunum in IUGR piglets via its substrate PGC1α. We also provide a novel insight into the effects of DMG-Na on jejunum redox status and mitochondrial function in IUGR piglets via the SIRT1/PGC1α pathway during the suckling period.

Methods

This trial was conducted in accordance with the Chinese guidelines for animal welfare and the experimental protocols for animal care approved by the Nanjing Agricultural University Institutional Animal Care and Use Committee.

Experimental design

This work was performed at the Yangzhou Fangling Agricultural and Pastoral Co., Ltd. (Jiangsu, China). Twenty-three normal birth weight (NBW) newborn piglets (1.53 ± 0.04 kg) and twenty-three IUGR newborn piglets (0.76 ± 0.06 kg) were selected from thirteen sows [Duroc × (Landrace × Yorkshire)] [12]. All selected piglets were similar in birth order (3rd or 4th) and all sows were fed the same gestating diet, which met the National Research Council (NRC, 2012) nutrient requirements.

In brief, one NBW and one IUGR newborn piglet were collected from each litter of three sows, and a total of three NBW and three IUGR piglets were slaughtered at birth for the transcriptome sequencing study. In addition, two NBW and two IUGR newborn piglets were collected from the litters of another ten sows, and one of each pair was assigned to the appropriate (NBW or IUGR) treatment and control groups. In total, 20 NBW piglets were allocated to the N (basic milk diet) and ND (basic milk diet supplemented with 0.1% DMG-Na) groups, and 20 IUGR piglets were assigned to the I (basic milk diet) and ID (basic milk diet supplemented with 0.1% DMG-Na) groups. The piglets were sustained on these diets from day 7 to day 21. DMG-Na was obtained from Qilu Sheng Hua Pharmaceutical Co., Ltd., Shandong, China.

The piglets were weighed at 0, 7, 10, 13, 16, 19, and 21 days of age. The piglets were fed warm milk collected from their corresponding sows every 2–3 h (approximately 9–10 times daily). Each sow was specially equipped with an experienced staff member to collect their milk and record their piglets' weights. Before the trial the sows were conditioned to touching by their staff member in order to reduce

unnecessary stress responses. After collection, milk was immediately moved to a constant-temperature water tank and measured using a plastic volumetric cylinder. We measured the milk that was supplied and the milk that remained after each feeding from day 7 to day 21, and calculated the absolute intake (intake = supplied - remained) at each feeding time. We fed piglets from individual bottles for 14 days in order to mimic natural feeding conditions. We calculated the average body weight gain (ADG), average feed intake (ADFI), and gain-to-feed ratio from day 7 to day 21. We calculated the diarrhea rates of piglets during the suckling period using the following formula:

$$\mathrm{Diarrhearate} = \frac{\mathrm{Sumofdiarrheapigletsoneachday}}{\mathrm{Numberoftrialpiglets} \times \mathrm{Numberoftrialdays}} \times 100\%$$

All piglets were housed in plastic enclosures (1.5 m × 0.7 m × 0.7 m; ambient temperature 33 °C) and were provided with water *ad libitum*.

Sample collection

Three newborn NBW piglets and three newborn IUGR piglets were stunned by electric shock and slaughtered by jugular bloodletting within 2 h after birth and without feeding. Samples were collected from their small intestines (duodenum, jejunum, ileum) and were stored in sterile containers, sealed, and immediately transferred to an anaerobic chamber. They were manually homogenized, subdivided into sterile tubes, and used for transcriptome sequencing and other analyses (see below). At 21 days of age, the remaining 40 piglets were weighed and slaughtered, and samples were collected from their small intestines. The small intestine was removed from the abdominal cavity and was divided into the duodenum (approx. the first 10 cm after the stomach), jejunum (approx. half of the small intestine below the duodenum), and ileum (the left part of the small intestine). Two 1 cm segments were sampled from each section. One sample was fixed in 4% buffered formaldehyde, and the other was fixed in 2.5% buffered glutaraldehyde. The samples were stored at -80°C until analysis.

Histological morphology assay

Small intestinal samples fixed in 4% buffered formaldehyde were dried using a graded series of xylene and ethanol, and then embedded in paraffin for histological processing. The samples (8 μm in size) were deparaffinized using xylene and rehydrated with graded dilutions of ethanol. Slides were stained with hematoxylin and eosin (HE). Ten slides from each sample (extracted from the middle of the sample) were prepared and viewed using an optical binocular microscope. Villus length (L) and width (W) and crypt depth were from five villi and crypts per slide [5]. The villus area (S) was calculated using the following formula:

$$\mathrm{S} = \pi \times \left(\frac{\mathrm{W}}{2}\right)\sqrt{\left(\frac{\mathrm{W}}{2}\right)^2 \square \mathrm{L}^2}$$

Redox status assay

Small intestine samples were homogenized in 0.9% sodium chloride solution on ice and centrifuged at 3,500 × *g* for 15 min at 4°C. The levels of superoxide dismutase (SOD, A001-2-1), glutathione peroxidase (GSH-Px, A005-1-2), glutathione (GSH, A005-1-2), catalase (CAT, A007-2-1), and malondialdehyde (MDA, A003-1-2) were measured from the supernatant of the tissue homogenate solution according to a previously described method with corresponding assay kits (Nanjing Jiancheng Bioengineering Institute, Nanjing, Jiangsu, China). Protein content was determined using a bicinchoninic acid (BCA, A045-3-2) protein assay kit (Nanjing Jiancheng Bioengineering Institute, Nanjing, Jiangsu, China).

Mitochondrial redox status assay

Small intestinal mitochondria were described previously [13]. The levels of protein content, manganese superoxide dismutase (MnSOD, A001-2-1), glutathione peroxidase (GPx, A005-1-2), GSH (A005-1-2), and γ-glutamylcysteine ligase (γ-GCL, A120-1-1) were measured according to a previously described method with corresponding assay kits (Nanjing Jiancheng Bioengineering Institute, Nanjing, Jiangsu, China).

Oxidative damage assay

ROS levels were detected using an ROS assay kit (E004-1-1, Nanjing Jiancheng Bioengineering Institute, Nanjing, Jiangsu, China). The results were expressed as the mean DCFH-DA fluorescence intensity of the sample over that of the control. Protein oxidation of intestinal mitochondria was calculated using the concentration of protein carbonyls (PC) and presented as nmol/mg protein. The level of 8-hydroxy-2-deoxyguanosine (8-OHdG, H165) in intestinal mitochondria was calculated in triplicate with an assay kit (Nanjing Jiancheng Bioengineering Institute, Nanjing, Jiangsu, China) according to the manufacturer's instructions, and presented in ng/mg protein.

MMP levels were calculated methods described in Hao et al., [14]. Briefly, the mitochondria were loaded with 1 × JC-1 dye at 37°C for 20 min, and then analyzed using flow cytometry (FACS Aria III). The results were calculated as the ratio of the fluorescence of aggregates (red) to that of the monomers (green).

The number of apoptotic and necrotic cells was measured using an Alexa Fluor® 488 Annexin V/Dead Cell Apoptosis kit (Thermo Fisher Scientific, Inc., Waltham, MA, USA). Briefly, the small intestine samples were ground using a glass homogenizer and their cells were washed twice with cool PBS buffer (pH = 7.4) and resuspended (2% suspension) in 1 × annexin-binding buffer. Then, the cell density was determined and the sample diluted in 1 × annexin binding buffer to 1×10^6 cells/mL. A sufficient volume of the cell suspension was stained with Annexin V-fluorescein isothiocyanate and propidium iodide (1:9 dilution) staining solution in darkness and at room temperature for 15 min. After incubation, the forward scatter of cells was determined, and Annexin V fluorescence intensity was measured in FL-1 with an excitation wavelength of 488 nm and an emission wavelength of 530 nm on a FACS Caliber (BD Biosciences).

The concentration of cellular adenosine triphosphate (ATP) in the small intestine was determined Zhang et al., [15]. The mtDNA copy number in the small intestine was determined using a real-time fluorescence quantitative polymerase chain reaction (PCR) kit (Tli RNaseH Plus; Takara Bio, Inc., Otsu, Japan) [16]. In brief, 20 μL PCR mixture consisting of 10 μL SYBR Premix Ex Taq (2×), 0.4 μL upstream primer, 0.4 μL

downstream primer, 0.4 μL ROX dye (50×), 6.8 μL ultrapure water, and 2 μL cDNA template was used. The sequence of the Mt $_{D\text{-}loop}$ gene upstream primer was 5'-AGGACTACGGCTTGAAAAGC-3', the sequence of the downstream primer was 5'-CATCTTGGCATCTTCAGTGCC-3', and the length of the target fragment was 198 bp. The sequence of the β-actin upstream primer was 5'-TTCTTGGGTATGGAGTCCTG-3', the sequence of the downstream primer was 5'-TAGAAGCATTTGCGGTGG-3', and the length of the target fragment was 150 bp. Each small intestine sample was amplified in triplicate. The fold-expression of each gene was calculated according to the $2^{-\Delta\Delta Ct}$ method [17], in which β-actin was used as an internal standard.

Construction of mRNA library and bioinformatic analysis assay

Total RNA was isolated from the jejunum samples using TRIzol (Invitrogen, Carlsbad, CA, USA) according to the manufacturer's instructions [17]. The double-stranded and single-stranded DNA in the total RNA was removed using DNase I digestion. The rRNA was removed using the RNase H or the Ribo-Zero method (Illumina, USA), and the purified mRNA was fragmented into small pieces with fragment buffer. First-strand and second-strand cDNA was generated in the First-Strand Reaction System using PCR. The reaction product was purified using magnetic beads, and A-Tailing Mix and RNA Index Adapters were added by incubation to carry out end repair. The cDNA fragments with adapters were amplified using PCR, and the products were purified using Ampure XP Beads. The library was validated using an Agilent Technologies 2100 bioanalyzer for quality control. The double-stranded PCR products were denatured and circularized by the splint oligo sequence. Single-stranded circular DNA (ssCir DNA) was used as the final library. The final library was amplified with phi29 (Thermo Fisher Scientific, MA, USA) to make a DNA nanoball (DNB), which contained more than 300 copies of one molecule. DNBs were then loaded into the patterned nanoarray, and single-end 50 base reads were generated on the BGISEQ500 platform (BGI-Shenzhen, China).

The sequencing data were filtered with SOAPnuke (v1.5.2) by removing reads of sequencing adapters, reads of low-quality base ratio more than 20%, and reads of unknown base ('N' base) ratio more than 5%, and the clean reads were stored in FASTQ format. The clean reads were then mapped to Sus_scrofa (NCBI_GCF_000003025.6_Sscrofa11.1) using HISAT2 (v2.0.4). Bowtie2 (v2.2.5) was applied to align the clean reads, and the expression levels of genes were calculated using RSEM (v1.2.12). The heatmap was drawn using pheatmap (v1.0.8) according to gene expression in different samples. Differential expression analysis was performed using DESeq2 (v1.4.5) with a $q < 0.05$. To gain insight into changes in phenotype, GO (http://geneontology.org/) and KEGG (https://www.kegg.jp/) enrichment analyses of differentially expressed annotated genes were performed using Phyper (https://en.wikipedia.org/wiki/Hypergeometric_distribution.) based on a hypergeometric test. The significance of enriched KEGG terms in the input list of differentially expressed genes compared to the whole genome background was determined using the corrected *P*-value < 0.05 as a threshold. The *P*-value was calculated as follows:

$$P = 1 - \sum_{i=0}^{m-1} \left(\frac{\binom{M}{i}\binom{N-M}{n-i}}{\frac{N}{n}} \right)$$

where N represents the number of KEGG annotated genes in jejunum samples, n represents the number of differentially expressed genes in N, M represents the number of particular KEGG annotated genes in a genome, and m represents the number of particular KEGG annotated genes expressed differentially in M. After correction for multiple testing, we chose pathways with a *P*-value < 0.05 to represent those significantly enriched in differentially expressed genes.

Weighted gene co-expression network analysis (WGCNA) assay

The *WGCNA* R package [18] was used to assess the relationships between clusters of co-expressed genes and phenotypes related to IUGR. To construct the network of co-expressed genes and to cluster genes that exhibited similar expression patterns, the *WGCNA* package built an adjacency matrix in which the nodes of the network corresponded to gene expression profiles. The edges between genes were determined using pairwise Pearson's correlations between gene expressions. First, it was necessary to find an optimal soft-thresholding power to transform the co-expression similarity into adjacency. After analyzing the network topology for several soft-thresholding parameters, power 6 was chosen as the soft-thresholding power to reach a scale-free topology index. Then, the gene network was constructed using the blockwiseModules function with a minimum module size of 30, and modules of co-expressed genes were detected using hierarchical clustering. Once groups of genes were characterized by expression profiles, it was necessary to detect modules that were most significantly related to the measured traits of interest. The associations between the modules and traits were quantified using Pearson's correlation. In particular, to identify the module-trait relationship, the *WGCNA* package determined the expression value of each module using principal component analysis. Module expression (ME) can be considered representative of the gene expression profile of the corresponding module. This approach allowed us to calculate Pearson's correlations between each module eigengene and trait, and thus to identify the module-trait relationship. The most significantly correlated eigengene was characterized by an absolute value of module-trait correlation > 0.8. Differential expression analysis was performed using DEGseq with $q \leq 0.01$, and the absolute value of Log2Ratio ≥ 1 as the default threshold to judge the significance of the difference. To annotate gene functions, all target genes were aligned against the Kyoto Encyclopedia of Genes (KEGG) and Gene Ontology (GO). GO and KEGG enrichment analyses of target genes were performed using the phyper [19] function in R. The *P*-value was corrected using the Bonferroni method, and a corrected *P*-value ≤ 0.05 was used as a threshold. GO or KEGG terms fulfilling this condition were defined as significantly enriched terms.

Quantitative real-time PCR assay

Quantitative real-time PCR (qPCR) was performed *sensu* Mohamed et al. [17]. Total RNA was extracted from jejunum samples using Trizol Reagent (TaKaRa, Dalian, China) and then reverse-transcribed using a commercial kit (Perfect Real Time, SYBR@ PrimeScript™, TaKaRa) following the manufacturer's instructions. The mRNA expression levels of specific genes were quantified via real-time PCR using SYBR@ *Premix Ex Taq*™ II (Tli RNaseH Plus) and an ABI 7300 Fast Real-Time PCR detection system (Applied Biosystems, Foster City, CA). The SYBR Green PCR reaction mixture consisted of 10 μL SYBR@ *Premix Ex Taq* (2×), 0.4 μL of the forward and reverse primers, 0.4 μL of ROX reference dye (50×), 6.8 μL of ddH_2O, and 2 μL of cDNA template. Each sample was amplified in triplicate. The fold-expression of each gene was calculated using the $2^{-\Delta\Delta Ct}$ method [17] with the *β-actin* gene as an internal standard. The primer sequences used are shown in **Table S1**.

Western blot assay

Total protein was isolated from the jejunum samples using a radioimmunoprecipitation assay lysis buffer containing a protease inhibitor cocktail (Beyotime Institute of Biotechnology, Jiangsu, China). The nuclear protein in the LM samples was extracted using a nuclear protein extraction kit (Beyotime Institute of Biotechnology, Jiangsu, China). The concentrations of total cellular and nuclear proteins in the LM samples were measured using a bicinchoninic acid protein assay kit (Beyotime Institute of Biotechnology, Jiangsu, China). Antibodies against related proteins were purchased from Cell Signaling Technology (Danvers, MA, USA). Equal quantities of protein were resolved by SDS-PAGE and then transferred onto polyvinylidene difluoride membranes. The membranes were then incubated with blocking buffer (5% bovine serum albumin in Tris-buffered saline containing 1% Tween 20) for 1 h at room temperature and probed with primary antibodies (1:1000) against Nrf2 (# 12721S), HO1 (# 82206S), SOD (# 37385S), GSH-Px (# 3286S), Sirt1 (# 9475S), PGC1α (# 2178S), OCLN (# 91131S), ZO1 (# 13663S), Cyt C (# 11940S), mtTFA (# 8076S), Mfn2 (# 9482S), Drp1 (# 8570S), Fis1 (# 84580S), and α-Tubulin (# 2125S) overnight at 4°C. Then, the membranes were washed with Tris-buffered saline with 0.05% Tween-20 and incubated with a suitable secondary antibody for 1 h at room temperature. Finally, the blots were detected using enhanced chemiluminescence reagents (ECL-Kit, Beyotime, Jiangsu, China), followed by autoradiography. Photographs of the membranes were taken using the Luminescent Image Analyzer LAS-4000 system (Fujifilm Co.) and quantified with ImageJ 1.42 q software (NIH, Bethesda, MD, USA).

Statistical analysis

Modeling of body weight data with repeated records (10 piglets per group) during the suckling period was conducted using a mixed model with group (G), time (T), DMG-Na (D), G × T, G × D, T × D, and G × T × D as fixed effects, and piglets as random effects. If the *P* value of G × T × D was < 0.05, the body weight among the different groups on each day was modeled using one-way ANOVA. Different superscripts (a, b, and c) indicate significant differences ($P < 0.05$). Small intestinal histological morphology, small intestinal redox status, and mitochondrial redox status among trial A (NBW, IUGR), trial B (NBW, IUGR, N, I), and trial C (N, ND, I, ID) were analyzed separately. For trial A, the data were analyzed using a mixed model with group (GA), intestine (IA), and GA × IA as fixed effects and piglets as random effects. If the *P* value of GA × IA was < 0.05, a paired t-test was used to compare the different groups in each segment of

the small intestine. For trial B, the data were analyzed using a mixed model with group (GB), time (T), intestine (IB), GB × T, GB × IB, T × IB, and GB × T × IB as fixed effects, and piglets as random effects. If the *P* value of the GB × T × IB was < 0.05, a one-way ANOVA was used to compare the different groups in each segment of the small intestine. For trial C, the corresponding data were analyzed using a mixed model with group (GC), DMG-Na (D), intestine (IC), GC × D, GC × IC, D × IC, and GC × D × IC as fixed effects, and piglets as random effects. If the *P* value of tGC × D × IC was < 0.05, a one-way ANOVA was used to compare the different groups in each segment of the small intestine.

The data on jejunum gene expression and protein expression among trials A, B, and C were also analyzed separately. For trial A, NBW and IUGR piglets were compared using a paired t-test. For trial B, the data were analyzed using a mixed model with group (GB), time (T), and GB × T as fixed effects and piglets as random effects. If the *P* value of GB × T was < 0.05, a one-way ANOVA was used to compare the different groups. For trial C, the data were analyzed using a mixed model with group (GC), DMG-Na (D), and GC × D as fixed effects, and piglets as random effects. If the *P* value of GC × D was < 0.05, a one-way ANOVA was used to compare the different groups. The values with different superscripts * (NBW, IUGR group in black color), and a, b, c, d (NBW, IUGR, N, I group in red color), and A, B, C, D (N, ND, I, ID group in blue color) were significantly different. All data were analyzed using Statistical Analysis System software (version 9.1; SAS Institute, Inc., Cary, NC, USA). Data are expressed as the mean ± standard deviation.

Results

Growth performance

Dietary DMG-Na supplementation improved the growth performance of IUGR piglets during the suckling period (**Fig. 1 and** Table 1**)**. Throughout the trial, the body weights of all piglets increased as the piglets grew. The interaction effect (group × time × DMG-Na) was significant ($P < 0.001$). Throughout the trial, group I had significantly lower body weight (50.33%, 35.92%, 27.82%, 30.68%, 31.06%, 28.67%, 23.22%) than did group N. In addition, groups ND and ID had significantly higher body weight [(26.07%, 29.68%, 18.07%, 15.83%, 15.43%) and (12.50%, 15.80%, 16.78%, 23.00%, 18.75%)] than did groups N and I, respectively. From day 7 to day 21 during the suckling period, the interaction effect (group × DMG-Na) was significant for ADG ($P = 0.009$), ADFI ($P = 0.017$) and diarrhea ($P < 0.001$). From day 7 to day 21 during the suckling period, group I had significantly lower ADG (12.77%) and ADFI (2.50%), but higher diarrhea (201.12%) than did group N. In addition, groups ND and ID had significantly higher ADG (28.01%, 30.08%), but lower ADFI (8.70%, 7.86%) and diarrhea (10.11%,

Table 1
Dietary DMG-Na supplementation improved the growth performance of IUGR piglets from day 7 to day 21 during the suckling period.[1]

	Groups[2]				*P* value		
Item[3]	N	ND	I	ID	P_G	P_D	$P_{G\times D}$
ADG (g/d)	282 ± 1.28[c]	361 ± 1.26[a]	246 ± 1.21[d]	320 ± 1.30[b]	< 0.001	< 0.001	0.009
ADFI (g/d)	494.73 ± 1.52[a]	451.67 ± 1.55[c]	482.35 ± 1.60[b]	444.44 ± 1.28[d]	< 0.001	< 0.001	0.017
G:F	0.57 ± 0.02	0.80 ± 0.03	0.51 ± 0.01	0.72 ± 0.01	< 0.001	< 0.001	0.397
Diarrhea (%)	0.89 ± 0.02[b]	0.80 ± 0.01[b]	2.68 ± 0.07[a]	0.89 ± 0.01[b]	< 0.001	< 0.001	< 0.001

[1] Data are expressed as the mean ± SD, n = 10. Different superscripts a, b, c, d (N, ND, I, ID group) represent significant differences ($P < 0.05$).

[2] NBW represents normal birth weight newborn piglets; IUGR represents intrauterine growth restriction newborn piglets; N represents NBW piglets fed a basic milk diet; ND represents NBW piglets fed a basic milk diet supplemented with 0.1% DMG-Na; I represents IUGR piglets fed a basic milk diet; ID represents IUGR piglets fed a basic milk diet supplemented with 0.1% DMG-Na.

3 ADG, average daily gain; ADFI, average daily feed intake; G:F, gain: feed intake.

Histological morphology assay

Dietary DMG-Na supplementation improved the histological morphology of the small intestine of IUGR piglets (**Figs. 2, 3)**. The interaction effect (groups × intestines) was significant for villus width ($P = 0.001$) and villus area ($P < 0.001$) in trial A. However, the interaction effects in trials B (groups × time × intestines) and C (groups × DMG-Na × intestines) were not significant ($P > 0.05$) for any of the tested histological morphology traits (villus length, villus width, crypt depth, and villus area). In trial A, small intestinal villus length, crypt depth, villus width [(25.93%, $P < 0.001$), (32.73%, $P < 0.001$), (28.00%, $P < 0.001$)], and villus area [(35.90%, $P < 0.001$), (42.55%, $P = 0.032$), 34.17%] in IUGR newborn piglets were decreased relative to NBW newborn piglets. In trial B, small intestinal villus length, crypt depth, and villus area were increased in the N and I groups relative to the NBW and IUGR groups, respectively. In addition, small intestinal villus length, crypt depth, villus width, and villus area were decreased in the I group relative to the N group. In trial C, small intestinal villus length, crypt depth, villus width, and villus area were increased in the ND and ID groups relative to the N and I groups, respectively.

Redox status assay

Dietary DMG-Na supplementation improved the redox status of the small intestine of IUGR piglets (**Fig. 4)**. The interaction effect (groups × intestines) was significant for GSH-Px ($P = 0.046$) and GSH ($P =$

0.016) in trial A. However, the interaction effects in trials B (groups × time × intestines) and C (groups × DMG-Na × intestines) were not significant ($P > 0.05$) for any of the tested redox status values (SOD, GSH-Px, GSH, CAT, and MDA). In trial A, decreases in small intestinal SOD, GSH-Px [(16.48%, $P = 0.046$), (0.43%, $P = 0.008$), (16.67%, $P = 0.002$)], GSH [(32.60%), (36.89%, $P = 0.001$), (31.62%, $P = 0.024$)], CAT, and an increase in small intestinal MDA were observed in IUGR newborn piglets relative to NBW newborn piglets. In trial B, increases in small intestinal SOD, GSH-Px, GSH, CAT, and MDA were observed in the N and I groups relative to the NBW and IUGR groups, respectively. In addition, a worse small intestinal redox status was found in the I group than in the N group. In trial C, an improvement in the small intestinal redox status was observed in the ND and ID groups relative to the N and I groups.

Mitochondrial redox status assay

Dietary DMG-Na supplementation improved the mitochondrial redox status of the small intestine of IUGR piglets (**Fig. 5)**. The interaction effects were not significant ($P > 0.05$) in any trial for any of the tested mitochondrial redox status values (MnSOD, GSPx, GSH, and γ-GCL). In trial A, the mitochondrial redox status of the small intestine was worse in IUGR newborn piglets than in NBW newborn piglets. In trial B, the mitochondrial redox status of the small intestine was increased in the N and I groups relative to the NBW and IUGR groups. In addition, a worse small intestine mitochondrial redox status was found in the I group than in the N group. In trial C, the mitochondrial redox status of the small intestine was increased in the ND and ID groups relative to the N and I groups.

Oxidative damage assay

Dietary DMG-Na supplementation improved the oxidative damage values in the small intestines of IUGR piglets (**Fig. 6)**. The interaction effects were not significant ($P > 0.05$) in any trial for any of the tested oxidative damage values (ROS, PC, 8-OHdG, MMP, apoptosis cells, necrotic cells, ATP, and mtDNA). In trial A, oxidative damage of the small intestine was enhanced in IUGR newborn piglets relative to NBW newborn piglets. In trial B, oxidative damage of the small intestine was increased in the N and I groups relative to the NBW and IUGR groups. In addition, the oxidative damage level in the small intestine was higher in the I group than in the N group. In trial C, small intestinal oxidative damage was improved in the ND and ID groups relative to the N and I groups.

RNA-seq and WGCNA assay

From the above results, we found that IUGR most affected the jejunum. Therefore, we identified the specific mechanism by which IUGR affected jejunum structure and function through RNA-seq and WGCNA methods.

To identify gene differentiation in the jejunum between the NBW and IUGR groups were constructed with total RNA and subjected to Illumina deep sequencing. Overviews of the sequencing and assembly results are presented in **Table S2**. After discarding the low-quality raw reads, 276,210,270 clean reads remained. All 19.935 assembled genes were referenced against the Swiss-Prot (12.630 genes; 63.36%), Nr (18.172 genes; 91.16%), Pfam (16.602 genes; 83.28%), KEGG (6.314 genes; 31.67%), KOG (10.976 genes; 55.06%),

and GO (7.487 genes; 37.56%) databases **(Table S3)**. To explore the molecular mechanisms of the jejunum in response to IUGR, RPKM analysis was performed to identify differentially expressed genes. We found that 14 mRNAs were upregulated ($P < 0.05$), while 25 genes were downregulated ($P < 0.05$) in response to IUGR **(Table S4)**. We then performed hierarchical clustering of the differentially expressed genes based on the six samples' log10 (RPKM + 1). The results indicated that the samples could be sorted into two distinct groups **(Fig. 7A)**. Overall, IUGR treatment had a significant impact on the global gene expression profile of the jejunum in newborn piglets.

According to the GO classification system, genes involved in "cellular processes" (25 genes) and "metabolic processes" (21 genes) were notably represented in the biological process category. Among the cellular components, "cell" (21 genes) was the most commonly represented, followed by "cell part" (21 genes), and "organelle" (15 genes). In the category of molecular function, a significant proportion of clusters were assigned to "binding" (21 genes) and "catalytic activity" (15 genes) **(Fig. S1)**. To classify orthologous gene products, the differentially expressed genes were subdivided into 25 KOG classifications. Among them, the cluster "General function prediction only" (10 genes) represented the largest group, followed by "Signal transduction mechanisms" (9 genes) and "Transcription" (4 genes) **(Fig. S2)**. The Kyoto Encyclopedia of Genes and Genomes (KEGG) classification was found for the differentially expressed genes that were further classified into six biochemical pathways, including cellular processes (5 genes), environmental information processing (17 genes), genetic information processing (2 genes), human diseases (31 genes), metabolism (10 genes), and organismal systems (50 genes) **(Fig. S3)**.

By performing the KEGG pathway analyses, a total of 15 pathways were identified that differed significantly ($P < 0.05$) between the IUGR newborn piglets and the NBW newborn piglets **(Fig. 7B)**. Among these pathways, "Bile secretion," "Pancreatic secretion," and "Salivary secretion" were included in the "Digestive system" sub-class. "Regulation of lipolysis in adipocytes" and "PPAR signaling pathway" were included in the "Endocrine system" sub-class. In addition, some important subclasses have been significantly enriched, including "Signal transduction," "Nervous system," "Metabolism of cofactors and vitamins," "Substance dependence," "Membrane transport," "Nervous system," "Immune system," "Folding, sorting and degradation," "Environmental adaptation," and "Endocrine system." These results imply that the genes involved in these pathways may play crucial roles in the jejunum of newborn piglets in response to IUGR.

The WGCNA analysis found nine modules (power = 12) **(Fig. S4)**. The 1,159 gene modules identified by WGCNA are shown in a cluster dendrogram **(Fig. S5)**, in which the branches correspond to modules and each leaf in the branch represents one probe. The *WGCNA* R package allowed us to quantify the correlations between genes in each module and the relevant phenotypes, thus quantifying the module-trait associations. Figure 7C shows module-trait associations using a heatmap plot, which graphically represents Pearson's correlation coefficients measured between every single module and trait **(Table S5)**. The yellow module ($P = 0.05$, $r = 0.81$) was most significantly correlated with the trait. According to the GO classification system, the 254 genes in the yellow module were involved in "cellular process" (65 genes),

and “single-organism process” (57 genes) were notably represented in the biological process category. Among the cellular components, “cell” (71 genes) and “cell part” (71 genes) were the most commonly represented, followed by “organelle” (50 genes). In the category of molecular function, a significant proportion of clusters were assigned to “binding” (73 genes) and “catalytic activity” (39 genes) **(Fig. S6)**. According to the KEGG classification, the 254 genes of the yellow module were further classified into four biochemical pathways **(Fig S7)**; cellular processes (25 genes), environmental information processing (59 genes), human diseases (58 genes), and organismal systems (118 genes). A total of 13 hub genes were obtained from the co-analysis of RNA-seq and WGCNA **(Table S6)**.

Gene expression

Dietary DMG-Na supplementation improved the jejunum redox status-related, cell adhesion-related, and mitochondrial function-related gene expression in IUGR piglets (**Fig. 8)**. There was a significant difference ($P < 0.05$) between the NBW and IUGR groups in trial A in redox status-related gene expression (*Nrf2*, *HO1*, *SOD1*, *GSH-Px*, *Sirt1*, *PGC1α*, *SOD2*, *γ-GCL*, *Trx2*, *Trx-R2*, *Prx3*), cell adhesion-related gene expression (*OCLN*, *CLDN2*, *CLDN3*, and *ZO1*), and mitochondrial function-related gene expression (*MCD*, *MCAD*, *SDH*, *UCP2*, *COX2*, *CS*, *COX1*, *Cyt C*, *ATP8*, *MHC1*, *mtTFA*, *Ndufa2*, *NRF1*, *UCP1*, *POLG1*, *POLG2*, *SSBP1*, *Drp1*, *Fis1*, and *Mfn2*). The interaction effect (groups × time) was significant for *Nrf2* ($P = 0.035$), *SOD1* ($P = 0.032$), *PGC1α* ($P = 0.028$), *SIRT1* ($P = 0.009$), *SOD2* ($P = 0.026$), *Trx-R2* ($P = 0.008$), *Prx3* ($P = 0.010$), *OCLN* ($P = 0.005$), *MCD* ($P = 0.002$), *MCAD* ($P = 0.014$), *SDH* ($P = 0.010$), *UCP2* ($P = 0.001$), *COX2* ($P = 0.010$), *CS* ($P = 0.011$), *COX1* ($P = 0.018$), *Cyt C* ($P = 0.038$), *ATP8* ($P = 0.016$), *MHC1* ($P = 0.046$), *mtTFA* ($P = 0.039$), *Ndufa2* ($P = 0.005$), *NRF1* ($P = 0.014$), *UCP1* ($P = 0.023$), *POLG1* ($P = 0.009$), *POLG2* ($P = 0.018$), *SSBP1* ($P = 0.007$), *Drp1* ($P = 0.010$), *Fis1* ($P = 0.009$), and *Mfn2* ($P = 0.012$) in trial B. In addition, the interaction effect (groups × time × intestines) was significant for *Prx3* ($P = 0.028$), *SDH* ($P = 0.031$), *UCP2* ($P = 0.008$), *COX2* ($P = 0.035$), *mtTFA* ($P = 0.036$), and *Mfn2* ($P = 0.049$) in trial C. In trial B, better values of redox status-related gene expression [among which, *Nrf2* (39.00%, 43.26%), *SOD1* (43.00%, 36.36%), *PGC1α* (43.00%, 33.93%), *SIRT1* (43.00%, 31.58%), *SOD2* (45.00%, 40.00%), *Trx-R2* (46.00%, 30.36%), and *Prx3* (46.00%, 32.76%) were significant], cell adhesion-related gene expression [among which, *OCLN* (43.00%, 22.41%) was significant], and mitochondrial function-related gene expression [among which, *MCD* (49.00%, 32.73%), *MCAD* (44.00%, 26.92%), *SDH* (47.00%, 29.41%), *UCP2* (46.00%, 24.53%), *COX2* (48.00%, 40.35%), *CS* (44.00%, 27.12%), *COX1* (48.00%, 37.10%), *Cyt C* (48.00%, 39.22%), *ATP8* (45.00%, 34.55%), *MHC1* (42.00%, 33.93%), *mtTFA* (49.00%, 45.28%), *Ndufa2* (48.00%, 21.05%), *NRF1* (48.00%, 28.85%), *UCP1* (46.00%, 26.79%), *POLG1* (46.00%, 27.12%), *POLG2* (45.00%, 31.37%), *SSBP1* (48.00%, 29.31%), *Drp1* (45.00%, 25.00%), *Fis1* (44.00%, 28.57%), and *Mfn2* (49.00%, 31.03%) were significant] were observed in N and I groups than in NBW and IUGR groups. In trial C, an improvement in redox status-related gene expression [among which, *Prx3* (29.45%, 23.38%) was significant], cell adhesion-related gene expression, and mitochondrial function-related gene expression [among which, *SDH* (23.81%, 16.67%), *UCP2* (27.40%, 19.70%), *COX2* (27.70%, 18.75%), *mtTFA* (26.85%, 19.48%) were significant] was observed in the ND and ID groups compared to the N and I groups.

Protein expression

Dietary DMG-Na supplementation improved the jejunum redox status-related, cell adhesion-related, and mitochondrial function-related protein expression in IUGR piglets (**Fig. 9)**. There was a significant difference ($P < 0.05$) between the NBW and IUGR groups in trial A in redox status-related protein expression (Nrf2, HO1, SOD, GSH-Px, Sirt1, and PGC1α), cell adhesion-related protein expression (OCLN and ZO1), and mitochondrial function-related protein expression (Cyt C, mtTFA, Mfn2, Drp1, and Fis1). The interaction effect (groups × time) was significant for Nrf2 ($P = 0.002$), SOD ($P < 0.001$), GSH-Px ($P = 0.014$), Sirt1 ($P = 0.004$), PGC1α ($P = 0.004$), OCLN ($P < 0.001$), ZO1 ($P < 0.001$), Cyt C ($P = 0.011$), mtTFA ($P = 0.041$), Mfn2 ($P = 0.037$), Drp1 ($P = 0.001$), and Fis1 ($P = 0.004$) in trial B. In addition, the interaction effect (groups × time × intestines) was significant for mtTFA ($P = 0.007$) in trial C. In trial B, better values of redox status-related protein expression [among which, Nrf2 (42.00%, 69.92%), SOD (59.00%, 20.97%), GSH-Px (51.00%, 48.15%), Sirt1 (62.00%, 52.94%), and PGC1α (63.00%, 46.15%) were significant], cell adhesion-related protein expression [among which, OCLN (59.00%, 31.48%) and ZO1 (58.00%, 39.22%) was significant], and mitochondrial function-related protein expression [among which, Cyt C (48.00%, 39.22%), mtTFA (35.00%, 33.96%), Mfn2 (52.00%, 46.15%), Drp1 (54.00%, 36.36%), and Fis1 (53.00%, 41.18%) were significant] were observed in N and I groups than in NBW and IUGR groups. In trial C, an improvement in redox status-related protein expression, cell adhesion-related protein expression, and mitochondrial function-related protein expression [among which, mtTFA (36.30%, 29.58%) was significant] was observed in the ND and ID groups compared to the N and I groups.

Discussion

IUGR has received attention from animal husbandry [1, 12, 20] because it causes irreversible oxidative damage, delayed postnatal growth, and damage to the small intestinal structure and function. Previous studies demonstrated poor performance and worse small intestinal structure and function in IUGR piglets [1, 2, 4]. These results are consistent with the current study, in which the I group showed lower growth performance than the N group. In addition, supplementation with DMG-Na improved the growth performance of IUGR piglets during the suckling period, perhaps as a result of its high antioxidant capacity and benefits on small intestinal health [21].

The small intestine is crucial for nutrient digestion, absorption, and metabolism. IUGR piglets usually experience severe intestinal diseases, and individuals are prone to feeding intolerance and digestive disease during the suckling period [22]. The movement of nutrients across the cell membrane depends on diffusion or active transport, which are regulated by small intestinal structure and function. In the present study, we found that ATP8, which is involved in maintaining mitochondrial function [23], was the most significantly changed gene in the jejunum between the NBW and IUGR groups. Thus, we hypothesized that jejunum dysfunction in IUGR piglets during the suckling period might be related to the alteration of mitochondrial function. Consistent with our results, studies have indicated that IUGR leads to intestinal villus atrophy, mucosal oxidative damage, and intestinal dysfunction, thereby causing diarrhea and reduction of feed utilization in piglets [24, 25]. This study also showed that autophagosomes and mitochondrial swelling appeared in the small intestines of the IUGR group. These may be related to malnutrition in utero, and are likely to be alleviated by replenishment of acquired nutrients [26]. A previous

study suggested that DMG-Na acted as an antioxidant, protecting the small intestine from oxidative damage and maintaining its normal histological morphology [27]. Another study found that DMG-Na exerted a positive effect on cell protection from oxidative damage [28], and this may be the reason for the results observed in the histological morphology test.

Oxidative damage can enhance ROS levels, decrease antioxidant capacity, and destroy small intestinal structure and function. The damaged small intestinal structure and function in the IUGR group in the current study suggests a destroyed redox status of the small intestine [29]. Oxidative damage can be improved by the SOD enzyme, which catalyzes the conversion of endogenous superoxide anions to hydrogen peroxide through disproportionation, and neutralized by the intracellular enzyme GSH-Px [30]. Meanwhile, the MnSOD enzyme, GSH-related metabolic enzyme, and γ-GCL enzyme are crucial in suppressing oxidative damage to mitochondria [31, 32]. A previous study found that DMG-Na could act as an antioxidant additive to improve antioxidant capacity [21, 27]. Our results suggest that adding 0.1% DMG-Na to the basic milk diet can improve antioxidant capacity by scavenging ROS generated excessively and thus maintaining the balance of the intracellular redox status.

ROS in cells maintains a dynamic balance with the antioxidant system. However, this balance is disturbed under certain conditions, resulting in oxidative damage [33]. Excessive ROS can induce mitochondrial and DNA structural damage, ultimately affecting antioxidant capacity. IUGR is closely related to oxidative damage, mitochondrial dysfunction, high ROS levels, and the occurrence of metabolic syndrome [34]. From the RNA-seq and WGCNA analyses in this study, we found that ATP8, which is involved in ROS generation [23], was the most significantly changed gene in the jejunum between the NBW and IUGR groups. It has been suggested that excessive ROS induces mitochondrial DNA (mtDNA) damage, impairs mitochondrial function, and produces more endogenous ROS [35]. The MMP level, which is negatively associated with ROS concentration, acts as an indicator of the beginning of mitochondria-dependent apoptosis. This is verified by the higher numbers of apoptotic and necrotic cells in the IUGR group than in the NBW group in this study [36]. The low level of ATP in this study may be caused by the destruction of mitochondrial structure and function, and it explains the low digestive function of the small intestine and low growth performance in the IUGR group compared to the NBW group. A previous study indicated that IUGR reduced antioxidant enzyme activity and mtDNA levels [37]. Another study also found that IUGR piglets have reduced antioxidant capacity and are prone to oxidative damage [38]. Similarly, in this study, reduction of antioxidant capacity lead to impaired intestinal function in the IUGR group relative to the NBW group. These results also suggested that DMG-Na could relieve oxidative damage by inhibiting excessive ROS generation, and previous studies verified that natural antioxidants could protect cells from oxidative damage.

Activation of Nrf2 and HO1 is important in relieving oxidative damage by regulating antioxidant gene expression (SDO, GSH-Px, γ-GCL) [39]. Mitochondria are rich in Trx2, Trx-R2, and Prx3 proteins, which act together to prevent oxidative damage by scavenging free radicals and regulating mitochondria-dependent apoptotic pathways [40]. PGC1α is a coactivator with pleiotropic functions that can regulate mitochondrial functional gene expression (COX1, Cyt C, ATP8, MHC1, mtTFA, Ndufa2, NRF1, NRF2, UCP1),

mtDNA replication and repair (POLG1, POLG2, SSBP1), and mitochondrial fission (Drp1, Fis1) and fusion (Mfn2) by inducing mitochondrial gene expression at the levels of both the nuclear and mitochondrial genomes [41, 42]. SIRT1, originally described as a factor regulating apoptosis and DNA repair, is highly sensitive to cellular redox and nutritional status and is known to control genomic stability and cellular metabolism [43]. Previous studies have reported that SIRT1 physically interacts with and deacetylates PGC1α at multiple lysine sites, consequently increasing PGC1α activity and regulating antioxidant capacity, lipid oxidation enzymes (MCD, MCAD), and mitochondrial gene expression (SDH, UCP2, COX2, CS) [44, 45]. ZO1, which is correlated with paracellular permeability, together with OCLN and CLDN gene families, is a key regulator of intestinal permeability [46]. To our knowledge, this is the first study to show that supplementation of DMG-Na improves growth performance and intestinal barrier functions in IUGR piglets during the suckling period via the SIRT1/PGC1α pathway, and further work is needed to better understand this specific mechanism.

Conclusions

The present study demonstrated that DMG-Na could effectively improve small intestinal damage in IUGR piglets during the suckling period. We speculated that DMG-Na could directly neutralize excessive free radicals and indirectly improve redox status and inhibit abnormal expression of stress-related factors via the SIRT1/PGC1α network. This suggests that DMG-Na can serve as a health-promoting substance and can be used for the prevention of small intestinal disorders in IUGR piglets during the suckling period.

Abbreviations

ADG: Average daily gain

ADFI: Average daily feed intake

ATP: Adenosine triphosphate

ATP8: Mitochondrially encoded ATP synthase membrane subunit 8

CAT: Catalase

CLDN2: Claudin 2

CLDN3: Claudin 3

COX1: Cytochrome c oxidase 1

COX2: Cytochrome c oxidase 2

CS: Citrate synthase

Cyt C: Cytochrome C

DMG-Na: Dimethylglycine sodium salt

Drp1: Dynamin-related protein 1

FBW: Final body weight

Fis1: Mitochondrial fission 1

GSH-Px: Glutathione peroxidase

GSH: Reduced glutathione

HO1: Heme oxygenase 1

IUGR: Intrauterine growth restriction

MCD: Malonyl-CoA decarboxylase

MCAD: Medium-chain acyl-CoA dehydrog-enase

MDA: Malondialdehyde

Mfn2: Mitofusin-2

MHCI: Major histocompatibility complex I

MMP: Mitochondrial membrane potential

MnSOD: Mn superoxide dismutase

mtDNA: Mitochondrial deoxyribonucleic acid

mtTFA: Mitochondrial transcription factor A

NBW: Normal birth weight

Ndufa2: NADH dehydrogenase (ubiquinone) iron-sulfur protein 2

Nrf1: Nuclear respiratory factor 1

Nrf2: Nuclear respiratory factor 2

OCLN: Occludin

PC: Protein carboxyls

PGC1α: Peroxisome proliferator-activated receptor gamma coactivator 1-alpha

POLG1: γ DNA polymerases catalytic subunit

POLG2: γ DNA polymerases accessory subunit

Prx3: Peroxidase 3

ROS: Reactive oxygen species

SDH: Mitochondrial proteins succinate dehydrogenase

SIRT1: Sirtuin 1

SOD: Superoxide dismutase

SSBP1: Mitochondrial DNA single-strand binding protein

Trx2: Thioredoxin 2

Trx-R2: Thioredoxin reductase 2

UCP1: Uncoupling protein 1

UCP2: Uncoupling protein 2

WGCNA: Weighted gene co-expression network analysis

ZO1: Zonula occludens-1

8-OHdG: 8-hydroxy-2 deoxyguanosine

Declarations

Ethics approval and consent to participate

This trial was conducted in accordance with the Chinese guidelines for animal welfare and the experimental protocols for animal care approved by the Nanjing Agricultural University Institutional Animal Care and Use Committee.

Consent for publication

Not applicable

Availability of data and materials

The datasets used and/or analysed during the current study are available from the corresponding author on reasonable request.

Competing interests

The authors declare that they have no competing interests

Funding

This work was supported by the National Natural Science Foundation of China [31572418]; National key research and development program of China [2018YFD0501101]; and the National Natural Science Foundation of China [31802101].

Authors' contributions

B.KW. designed and wrote the manuscript and performed most experiments. B.K.W. and J.L.Y. contributed to bioinformatics and statistical analyses. B.K.W. performed some experiments and edited the manuscript. B.K.W., L.Q.M., Z.J.F., Z.L.L., and W.T. contributed to the design of the study and reviewed and edited the manuscript. All authors reviewed and take full responsibility for the contents of the manuscript. B.K.W. is the guarantor of this work and, as such, had full access to all the data in the study and takes responsibility for the integrity of the data and the accuracy of the data analysis.

Acknowledgements

Not applicable

References

1. Li T, Huang S, Lei L, Tao S, Xiong Y, Wu G, et al. Intrauterine growth restriction alters nutrient metabolism in the intestine of porcine offspring. J Anim Sci Biotechnol. 2021;12(1):15. doi:10.1186/s40104-020-00538-y.
2. Dong L, Zhong X, He J, Zhang L, Bai K, Xu W, et al. Supplementation of tributyrin improves the growth and intestinal digestive and barrier functions in intrauterine growth-restricted piglets. Clin Nutr. 2016;35(2):399–407. doi:10.1016/j.clnu.2015.03.002.
3. Xu W, Bai K, He J, Su W, Dong L, Zhang L, et al. Leucine improves growth performance of intrauterine growth retardation piglets by modifying gene and protein expression related to protein synthesis. Nutrition. 2016;32(1):114–21. doi:10.1016/j.nut.2015.07.003.
4. Chen Y, Zhang H, Chen Y, Jia P, Ji S, Zhang Y, et al. Resveratrol and its derivative pterostilbene ameliorate intestine injury in intrauterine growth-retarded weanling piglets by modulating redox status and gut microbiota. J Anim Sci Biotechnol. 2021;12(1):70. doi:10.1186/s40104-021-00589-9.
5. Dong L, Zhong X, Ahmad H, Li W, Wang Y, Zhang L, et al. Intrauterine growth restriction impairs small intestinal mucosal immunity in neonatal piglets. J Histochem Cytochem. 2014;62(7):510–8. doi:10.1369/0022155414532655.
6. Dillin A, Hsu AL, Arantes-Oliveira N, Lehrer-Graiwer J, Hsin H, Fraser AG, et al. Rates of behavior and aging specified by mitochondrial function during development. Science. 2002;298(5602):2398–401.

doi:10.1126/science.1077780.

7. Cheng K, Wang T, Li S, Song Z, Zhang H, Zhang L, et al. Effects of early resveratrol intervention on skeletal muscle mitochondrial function and redox status in neonatal piglets with or without intrauterine growth retardation. Oxid Med Cell Longev. 2020;2020:4858975. doi:10.1155/2020/4858975.
8. Feng C, Bai K, Wang A, Ge X, Zhao Y, Zhang L, et al. Effects of dimethylglycine sodium salt supplementation on growth performance, hepatic antioxidant capacity, and mitochondria-related gene expression in weanling piglets born with low birth weight. J Anim Sci. 2018;96(9):3791–803. doi:10.1093/jas/sky233.
9. Friesen RW, Novak EM, Hasman D, Innis SM. Relationship of dimethylglycine, choline, and betaine with oxoproline in plasma of pregnant women and their newborn infants. J Nutr. 2007;137(12):2641–6. doi:10.1093/jn/137.12.2641.
10. Bai K, Jiang L, Zhang L, Zhao Y, Lu Y, Zhu J, et al. In vitro free radical scavenging capacity of dimethylglycine sodium salt and its protective ability against oleic acid hydroperoxide-induced oxidative damage in IPEC-J2 cells. Int J Mol Med. 2018;42(6):3447–58. doi:10.3892/ijmm.2018.3876.
11. Bai K, Jiang L, Zhu S, Feng C, Zhao Y, Zhang L, et al. Dimethylglycine sodium salt protects against oxidative damage and mitochondrial dysfunction in the small intestines of mice. Int J Mol Med. 2019;43(5):2199–211. doi:10.3892/ijmm.2019.4093.
12. Wang T, Huo YJ, Shi F, Xu RJ, Hutz RJ. Effects of intrauterine growth retardation on development of the gastrointestinal tract in neonatal pigs. Biol Neonate. 2005;88(1):66–72. doi:10.1159/000084645.
13. Thomas S, Anup R, Susama P, Balasubramanian KA. Nitric oxide prevents intestinal mitochondrial dysfunction induced by surgical stress. Br J Surg. 2001;88(3):393–9. doi:10.1046/j.1365-2168.2001.01683.x.
14. Hao S, Zhang L, Li J. Anti-benzopyrene-7,8-diol-9,10-epoxide induces apoptosis via mitochondrial pathway in human bronchiolar epithelium cells independent of the mitochondria permeability transition pore. Food Chem Toxicol. 2012;50(7):2417. doi:10.1016/j.fct.2012.04.041.
15. Zhang J, Xu L, Zhang L, Ying Z, Su W, Wang T. Curcumin attenuates D-galactosamine/lipopolysaccharide-induced liver injury and mitochondrial dysfunction in mice. J Nutr. 2014;144(8):1211–8. doi:10.3945/jn.114.193573.
16. Bai P, Cantó C, Oudart H, Brunyánszki A, Cen Y, Thomas C, et al. PARP-1 inhibition increases mitochondrial metabolism through SIRT1 activation. Cell Metab. 2011;13(4):461–8. doi:10.1016/j.cmet.2011.03.004.
17. Mohamed JS, Lopez MA, Boriek AM. Mechanical stretch up-regulates microRNA-26a and induces human airway smooth muscle hypertrophy by suppressing glycogen synthase kinase-3β. J Biol Chem. 2010;285(38):29336–47. doi:10.1074/jbc.M110.101147.
18. Langfelder P, Horvath S. WGCNA: an R package for weighted correlation network analysis. BMC Bioinform. 2008;9:559. doi:10.1186/1471-2105-9-559.

19. Chin CH, Chen SH, Wu HH, Ho CW, Ko MT, Lin CY. cytoHubba: identifying hub objects and sub-networks from complex interactome. BMC Syst Biol. 2014;8(Suppl 4):11. doi:10.1186/1752-0509-8-s4-s11. Suppl 4) .
20. Garite TJ, Clark R, Thorp JA. Intrauterine growth restriction increases morbidity and mortality among premature neonates. Am J Obstet Gynecol. 2004;191(2):481–7. doi:10.1016/j.ajog.2004.01.036.
21. Bai K, Xu W, Zhang J, Kou T, Niu Y, Wan X, et al. Assessment of free radical scavenging activity of dimethylglycine sodium salt and its role in providing protection against lipopolysaccharide-induced oxidative stress in mice. PloS one. 2016;11(5):e0155393. doi:10.1371/journal.pone.0155393.
22. Bernstein IM, Horbar JD, Badger GJ, Ohlsson A, Golan A. Morbidity and mortality among very-low-birth-weight neonates with intrauterine growth restriction. Am J Obstet Gynecol. 2000;182(1):198–206. doi:10.1016/s0002-9378(00)70513-8.
23. Weiss H, Wester-Rosenloef L, Koch C, Koch F, Baltrusch S, Tiedge M, et al. The mitochondrial Atp8 mutation induces mitochondrial ROS generation, secretory dysfunction, and β-cell mass adaptation in conplastic B6-mtFVB mice. Endocrinology. 2012;153(10):4666–76. doi:10.1210/en.2012-1296.
24. Wang T, Huo YJ, Shi F, Xu RJ, Hutz RJ. Effects of intrauterine growth retardation on development of the gastrointestinal tract in neonatal pigs. Biol Neonate. 2005;88(1):66–72. doi:10.1159/000084645.
25. Wang J, Chen L, Li D, Yin Y, Wang X, Li P, et al. Intrauterine growth restriction affects the proteomes of the small intestine, liver, and skeletal muscle in newborn pigs. J Nutr. 2008;138(1):60–6. doi:10.1093/jn/138.1.60.
26. Minamikawa T, Williams DA, Bowser DN, Nagley P. Mitochondrial permeability transition and swelling can occur reversibly without inducing cell death in intact human cells. Exp Cell Res. 1999;246(1):26–37. doi:10.1006/excr.1998.4290.
27. Friesen RW, Novak EM, Hasman D, Innis SM. Relationship of dimethylglycine, choline, and betaine with oxoproline in plasma of pregnant women and their newborn infants. J Nutr. 2007;137(12):2641. doi:10.1093/jn/137.12.2641.
28. Look MP, Riezler R, Berthold HK, Stabler SP, Schliefer K, Allen RH, et al. Decrease of elevated N,N-dimethylglycine and N-methylglycine in human immunodeficiency virus infection during short-term highly active antiretroviral therapy. Metabolism. 2001;50(11):1275–81. doi:10.1053/meta.2001.27201.
29. Mizushima N. Mizushima N. Autophagy: process and function. Genes Dev. 2007;21(22):2861–73. doi:10.1101/gad.1599207.
30. Bayrak O, Uz E, Bayrak R, Turgut F, Atmaca AF, Sahin S, et al. Curcumin protects against ischemia/reperfusion injury in rat kidneys. World J Urol. 2008;26(3):285–91. doi:10.1007/s00345-008-0253-4.
31. Tang Y, Gao C, Xing M, Li Y, Zhu L, Wang D, et al. Quercetin prevents ethanol-induced dyslipidemia and mitochondrial oxidative damage. Food Chem Toxicol. 2012;50(5):1194–200. doi:10.1016/j.fct.2012.02.008.

32. Langston JW, Li W, Harrison L, Aw TY. Activation of promoter activity of the catalytic subunit of γ-glutamylcysteine ligase (GCL) in brain endothelial cells by insulin requires antioxidant response element 4 and altered glycemic status: implication for GCL expression and GSH synthesis. Free Radic Biol Med. 2011;51(9):1749–57. doi:10.1016/j.freeradbiomed.2011.08.004.
33. Sun X, Zemel MB. Leucine modulation of mitochondrial mass and oxygen consumption in skeletal muscle cells and adipocytes. Nutr Metab. 2009;6(1):26. doi:10.1186/1743-7075-6-26.
34. Biri A, Bozkurt N, Turp A, Kavutcu M, Himmetoglu O, Durak I. Role of oxidative stress in intrauterine growth restriction. Gynecol Obstet Invest. 2007;64(4):187–92. doi:10.1159/000106488.
35. Simmons RA. Developmental origins of diabetes: The role of oxidative stress. Free Radic Biol Med. 2006;40(6):917–22. doi:10.1016/j.freeradbiomed.2005.12.018.
36. Bazhin AA, Sinisi R, De Marchi U, Hermant A, Sambiagio N, Maric T, et al. A bioluminescent probe for longitudinal monitoring of mitochondrial membrane potential. Nat Chem Biol. 2020;16(12):1385–93. doi:10.1038/s41589-020-0602-1.
37. Yu YC, Kuo CL, Cheng WL, Liu CS, Hsieh M. Decreased antioxidant enzyme activity and increased mitochondrial DNA damage in cellular models of Machado-Joseph disease. J Neurosci Res. 2009;87(8):1884–91. doi:10.1002/jnr.22011.
38. Biri A, Bozkurt N, Kavutcu A, Himmetoglu M, Durak O. I. Role of oxidative stress in intrauterine growth restriction. Gynecol Obstet Invest. 2007;64(4):187. doi:10.1159/000106488.
39. Loboda A, Damulewicz M, Pyza E, Jozkowicz A, Dulak J. Role of Nrf2/HO-1 system in development, oxidative stress response and diseases: an evolutionarily conserved mechanism. Cell Mol Life Sci. 2016;73(17):3221–47. doi:10.1007/s00018-016-2223-0.
40. Yan BC, Park JH, Ahn JH, Lee YJ, Lee TH, Lee CH, et al. Comparison of the immunoreactivity of Trx2/Prx3 redox system in the hippocampal CA1 region between the young and adult gerbil induced by transient cerebral ischemia. Neurochem Res. 2012;37(5):1019–30. doi:10.1007/s11064-012-0702-8.
41. Chiu H, Brittingham JA, Laskin DL. Differential induction of heme oxygenase-1 in macrophages and hepatocytes during acetaminophen-induced hepatotoxicity in the rat: effects of hemin and biliverdin. Toxicol Appl Pharmacol. 2002;181(2):106–15. doi:10.1006/taap.2002.9409.
42. Hwang JW, Yao H, Caito S, Sundar IK, Rahman I. Redox regulation of SIRT1 in inflammation and cellular senescence. Free Radic Biol Med. 2013;61:95–110. doi:10.1016/j.freeradbiomed.2013.03.015.
43. Herskovits AZ, Guarente L. SIRT1 in neurodevelopment and brain senescence. Neuron. 2014;81(3):471–83. doi:10.1016/j.neuron.2014.01.028.
44. Lin J, Handschin C, Spiegelman BM. Metabolic control through the PGC-1 family of transcription coactivators. Cell Metab. 2005;1(6):361–70. doi:10.1016/j.cmet.2005.05.004.
45. St-Pierre J, Drori S, Uldry M, Silvaggi JM, Rhee J, Jäger S, et al. Suppression of reactive oxygen species and neurodegeneration by the PGC-1 transcriptional coactivators. Cell. 2006;127(2):397–408. doi:10.1016/j.cell.2006.09.024.

46. Rincon-Heredia R, Flores-Benitez D, Flores-Maldonado C, Bonilla-Delgado J, García-Hernández V, Verdejo-Torres O, et al. Ouabain induces endocytosis and degradation of tight junction proteins through ERK1/2-dependent pathways. Exp Cell Res. 2014;320(1):108–18. doi:10.1016/j.yexcr.2013.10.008.

Figures

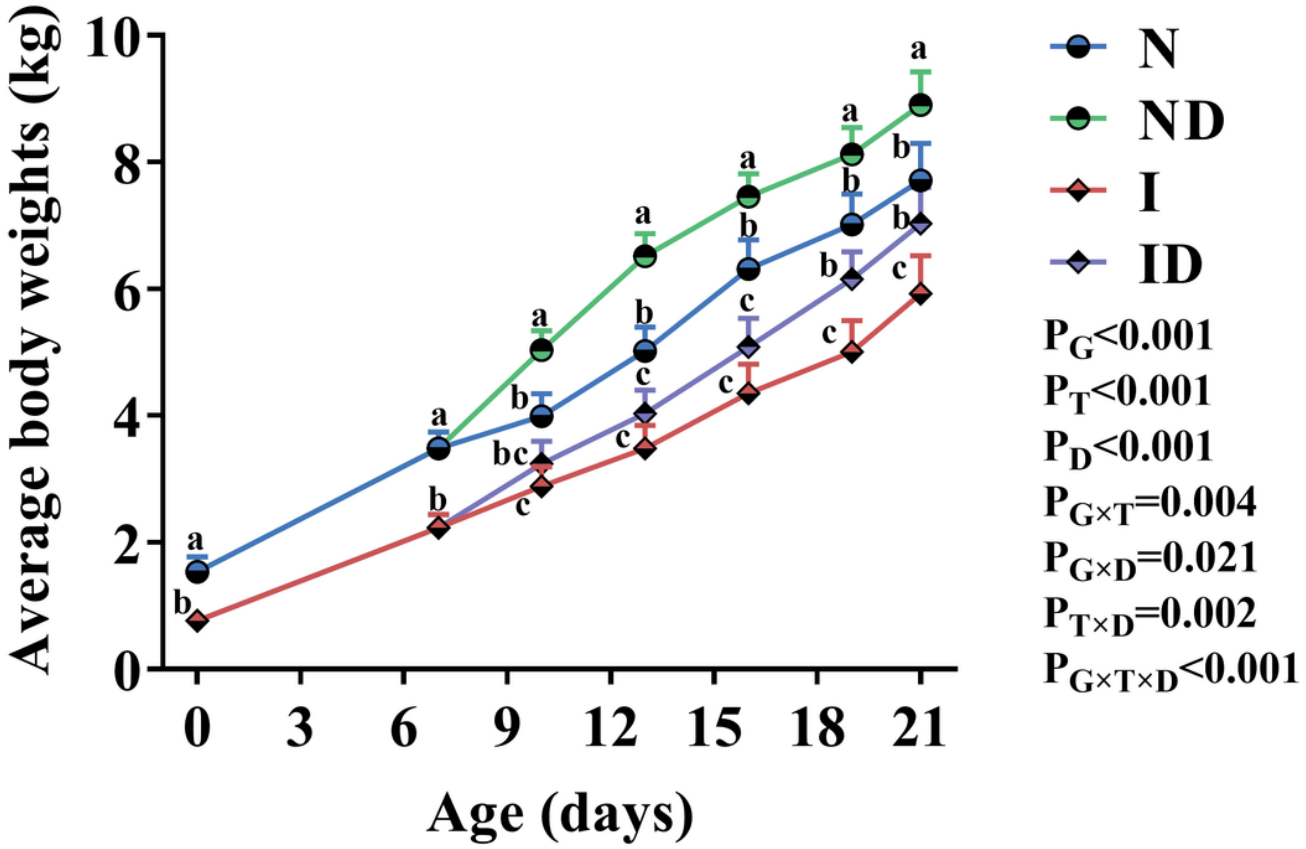

Figure 1

Dietary DMG-Na supplementation improved the growth performance of IUGR piglets during the suckling period. Data are expressed as the mean ± SD, n = 10. Different superscripts a, b, c (N, ND, I, ID group) represent significant differences ($P < 0.05$). NBW represents normal birth weight newborn piglets; IUGR represents intrauterine growth restriction newborn piglets; N represents NBW piglets fed a basic milk diet; ND represents NBW piglets fed a basic milk diet supplemented with 0.1% DMG-Na; I represents IUGR piglets fed a basic milk diet; ID represents IUGR piglets fed a basic milk diet supplemented with 0.1% DMG-Na.

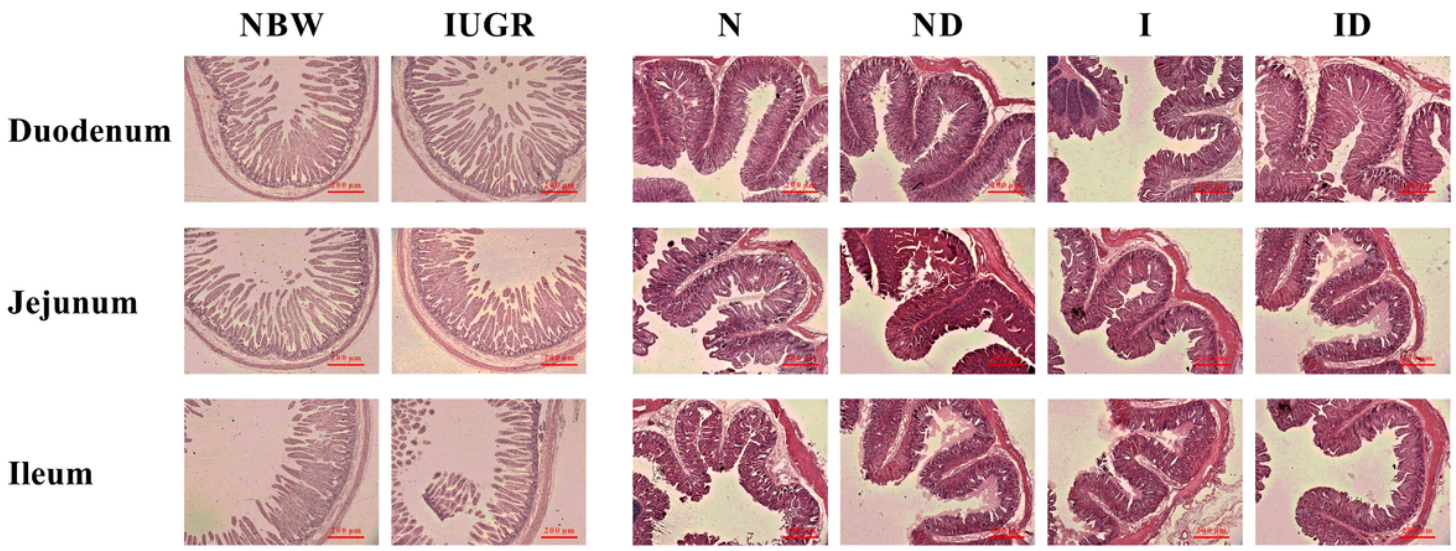

Figure 2

Dietary DMG-Na supplementation improved the histological morphology of the small intestine of IUGR piglets during the suckling period. Scale bars represent 200 μm. NBW represents normal birth weight newborn piglets; IUGR represents intrauterine growth restriction newborn piglets; N represents NBW piglets fed a basic milk diet; ND represents NBW piglets fed a basic milk diet supplemented with 0.1% DMG-Na; I represents IUGR piglets fed a basic milk diet; ID represents IUGR piglets fed a basic milk diet supplemented with 0.1% DMG-Na.

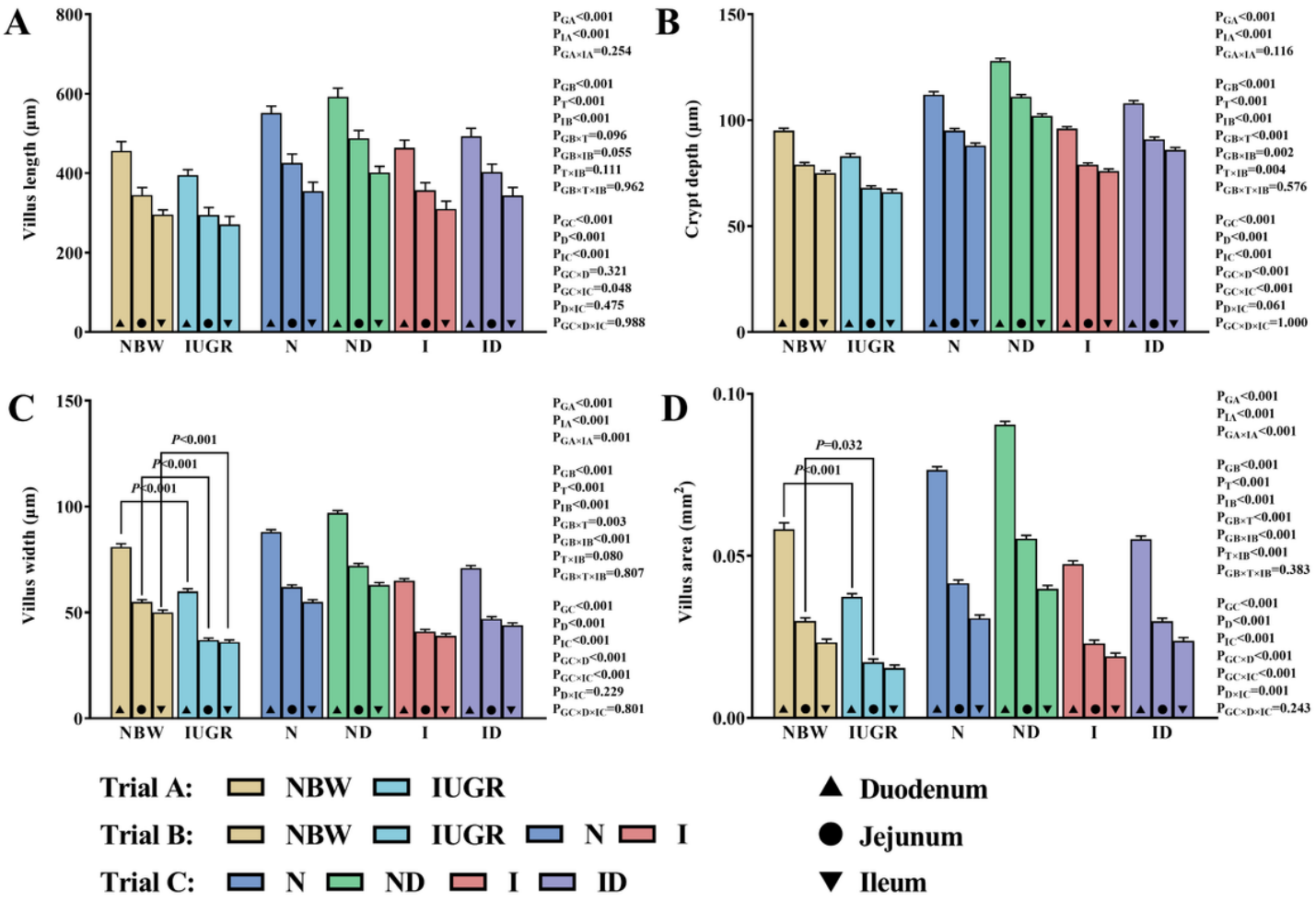

Figure 3

Dietary DMG-Na supplementation improved the histological morphology values of the small intestine of IUGR piglets during the suckling period. Data are expressed as the mean ± SD, n = 10. Different superscripts * (Trial A: NBW, IUGR group in black color), and a, b, c, d (Trial B: NBW, IUGR, N, I group in red color), and A, B, C, D (Trial C: N, ND, I, ID group in blue color) represent significant differences ($P < 0.05$). NBW represents normal birth weight newborn piglets; IUGR represents intrauterine growth restriction newborn piglets; N represents NBW piglets fed a basic milk diet; ND represents NBW piglets fed a basic milk diet supplemented with 0.1% DMG-Na; I represents IUGR piglets fed a basic milk diet; ID represents IUGR piglets fed a basic milk diet supplemented with 0.1% DMG-Na.

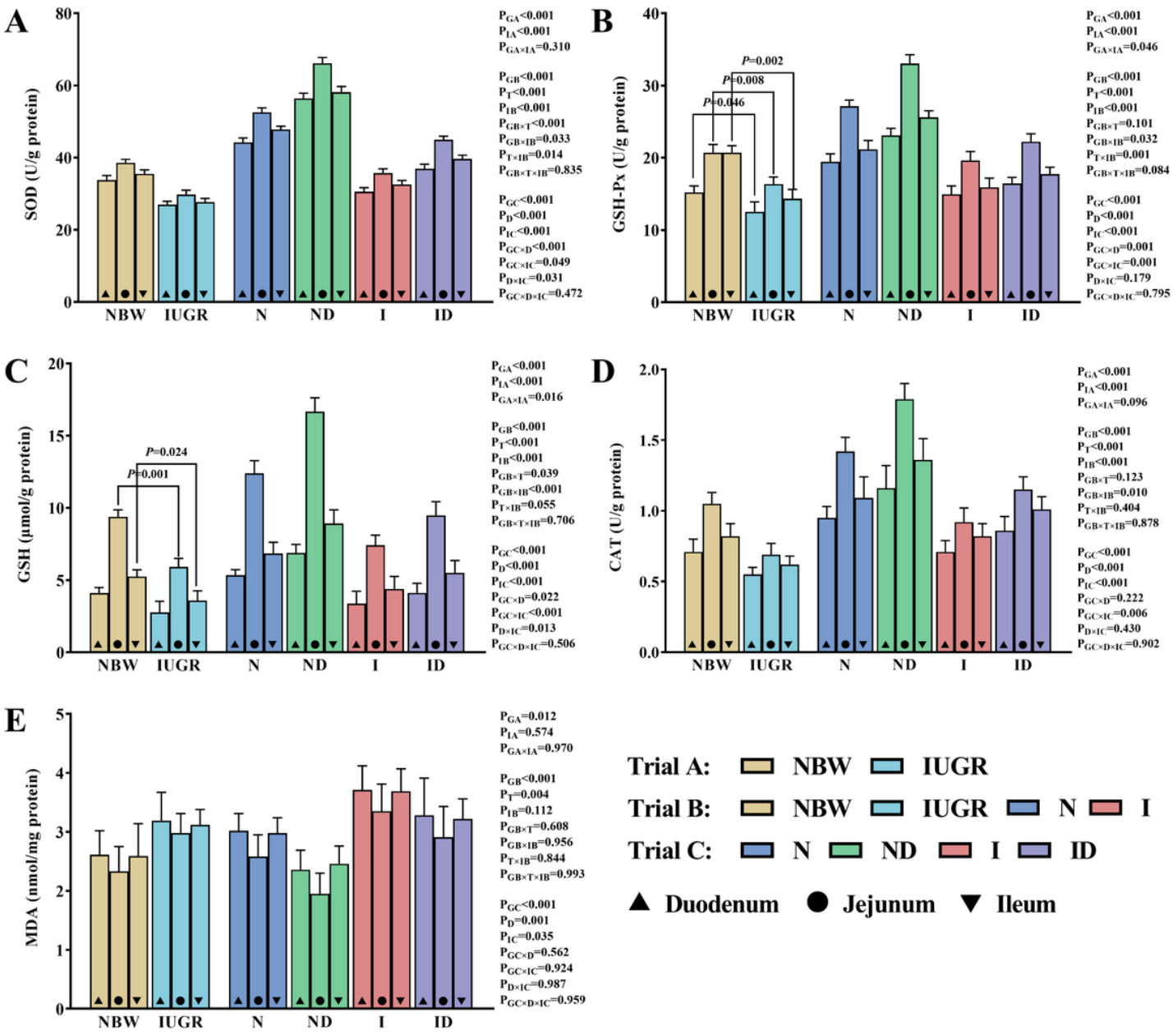

Figure 4

Dietary DMG-Na supplementation improved the redox status of the small intestine of IUGR piglets during the suckling period. Data are expressed as the mean ± SD, n = 10. Different superscripts * (Trial A: NBW, IUGR group in black color), and a, b, c, d (Trial B: NBW, IUGR, N, I group in red color), and A, B, C, D (Trial C: N, ND, I, ID group in blue color) represent significant differences ($P < 0.05$). NBW represents normal birth weight newborn piglets; IUGR represents intrauterine growth restriction newborn piglets; N represents NBW piglets fed a basic milk diet; ND represents NBW piglets fed a basic milk diet supplemented with 0.1% DMG-Na; I represents IUGR piglets fed a basic milk diet; ID represents IUGR piglets fed a basic milk diet supplemented with 0.1% DMG-Na. SOD, superoxide dismutase; GSH-Px, glutathione peroxidase; GSH, glutathione; CAT, catalase; MDA, methane dicarboxylic aldehyde.

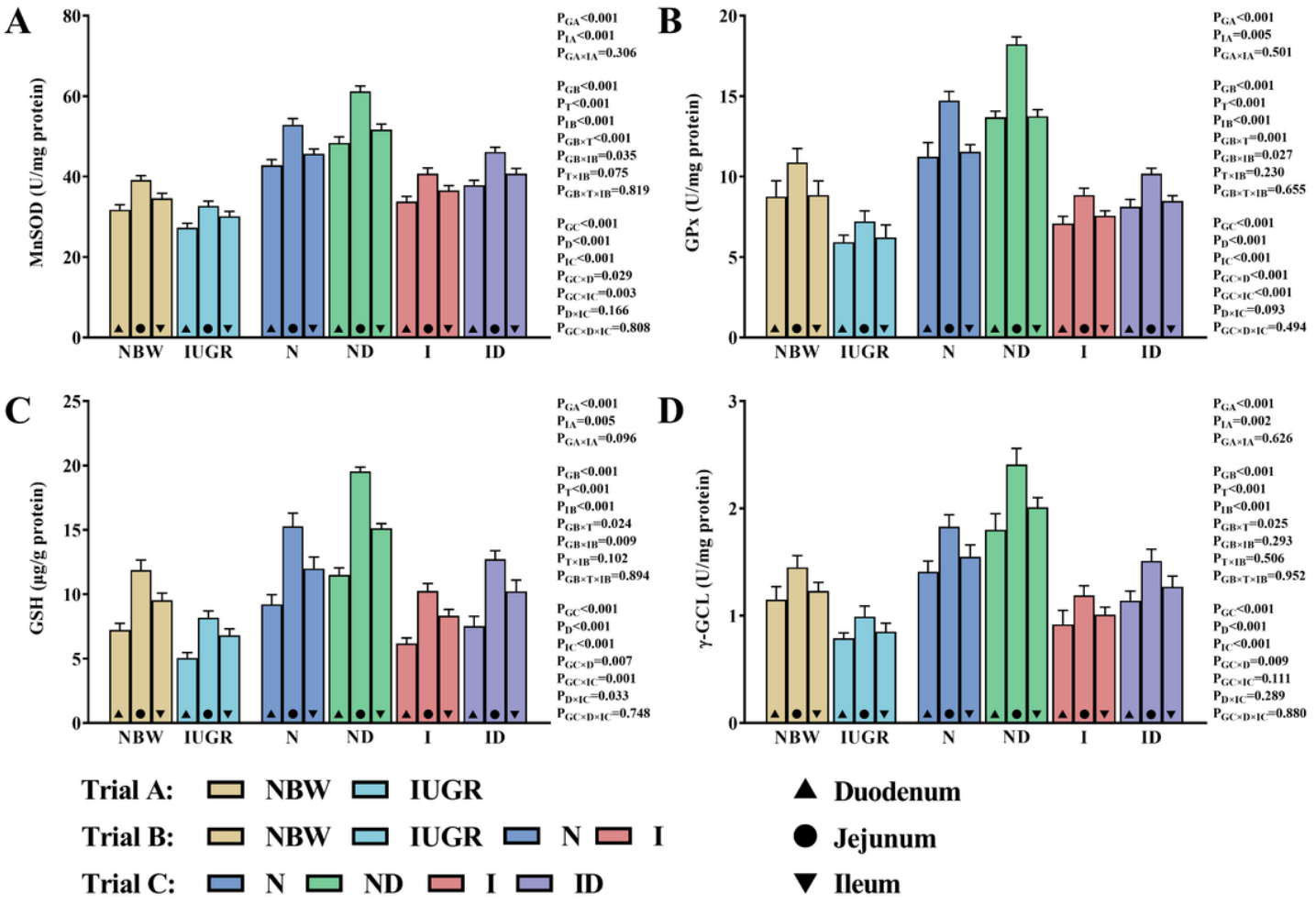

Figure 5

Dietary DMG-Na supplementation improved the mitochondrial redox status of small intestine of IUGR piglets during the suckling period. Data are expressed as the mean ± SD, n = 10. Different superscripts * (Trial A: NBW, IUGR group in black color), and a, b, c, d (Trial B: NBW, IUGR, N, I group in red color), and A, B, C, D (Trial C: N, ND, I, ID group in blue color) represent significant differences ($P < 0.05$). NBW represents normal birth weight newborn piglets; IUGR represents intrauterine growth restriction newborn piglets; N represents NBW piglets fed a basic milk diet; ND represents NBW piglets fed a basic milk diet supplemented with 0.1% DMG-Na; I represents IUGR piglets fed a basic milk diet; ID represents IUGR piglets fed a basic milk diet supplemented with 0.1% DMG-Na. MnSOD, manganese superoxide dismutase; GPx, glutathione peroxidase; GSH, glutathione; γ-GCL, γ-glutamylcysteine ligase.

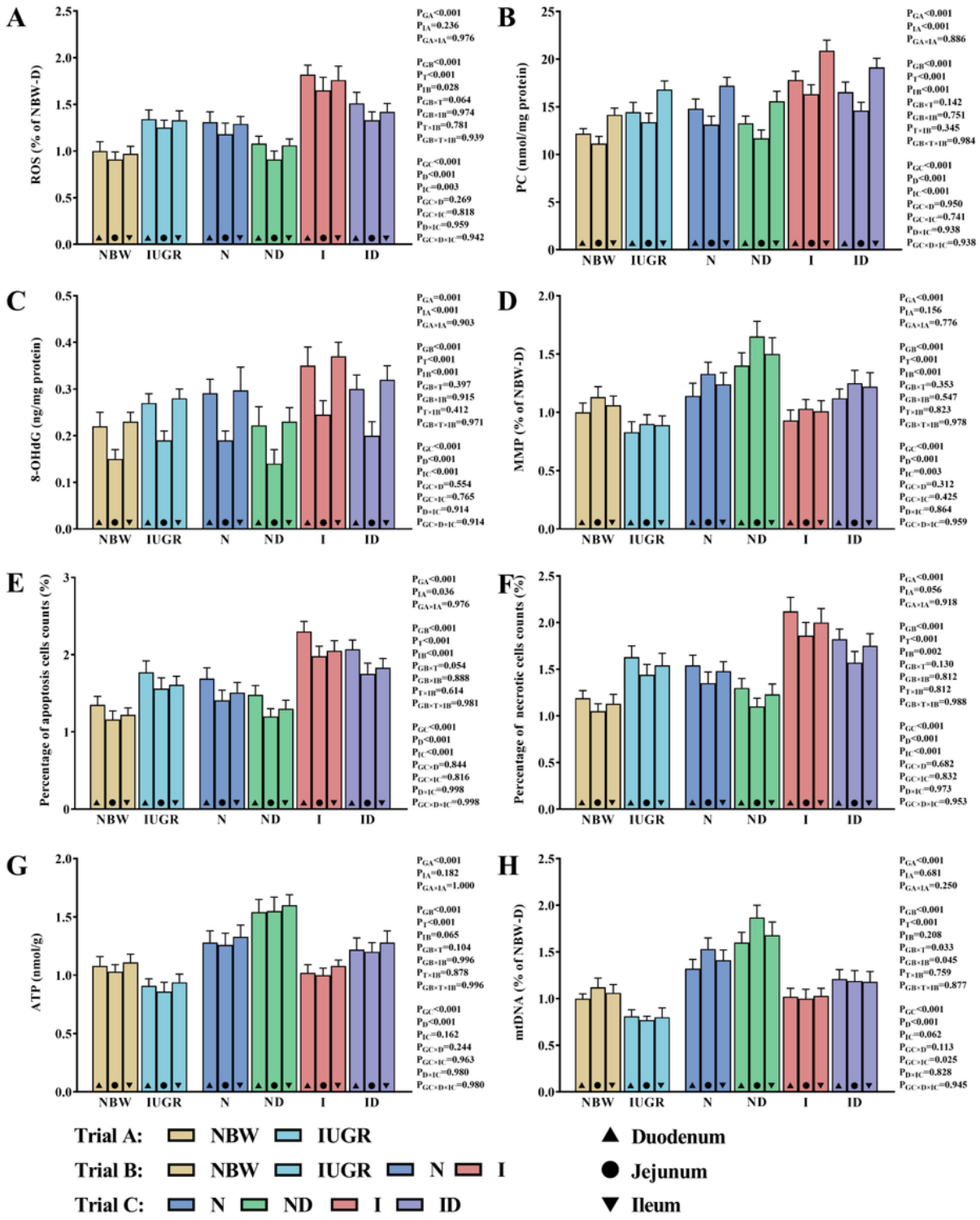

Figure 6

Dietary DMG-Na supplementation improved the oxidative damage values of small intestine of IUGR piglets during the suckling period. Data are expressed as the mean ± SD, n = 10. Different superscripts * (Trial A: NBW, IUGR group in black color), and a, b, c, d (Trial B: NBW, IUGR, N, I group in red color), and A, B, C, D (Trial C: N, ND, I, ID group in blue color) represent significant differences ($P < 0.05$). NBW represents normal birth weight newborn piglets; IUGR represents intrauterine growth restriction newborn piglets; N

represents NBW piglets fed a basic milk diet; ND represents NBW piglets fed a basic milk diet supplemented with 0.1% DMG-Na; I represents IUGR piglets fed a basic milk diet; ID represents IUGR piglets fed a basic milk diet supplemented with 0.1% DMG-Na. ROS, reactive oxygen species; PC, protein carbonyls; 8-OHdG, 8-hydroxy-2- deoxyguanosine; MMP, mitochondrial membrane potential; ATP, adenosine triphosphate; mtDNA, mitochondria DNA.

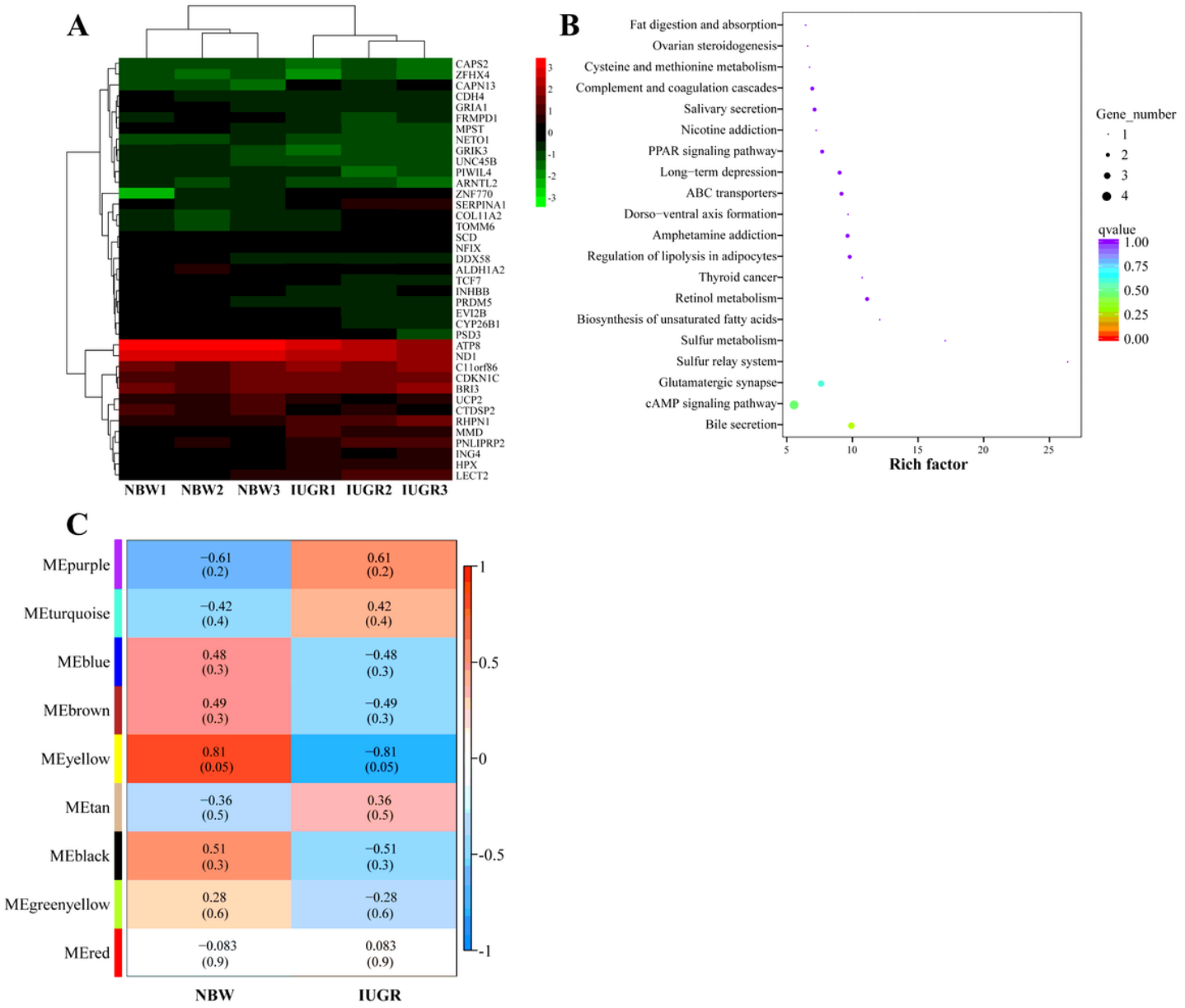

Figure 7

The RNA-seq analysis of jejunum of NBW and IUGR newborn piglets. The hierarchical clustering of the different expression genes from the RNA-seq analysis (n=3) (A), the KEGG pathway analyses (n=3) (B), the heatmap plot between modules and traits by WGCNA analysis (n=3) (C) of jejunum in NBW and IUGR newborn piglets. NBW, normal birth weight newborn piglets; IUGR, intrauterine growth restriction newborn piglets.

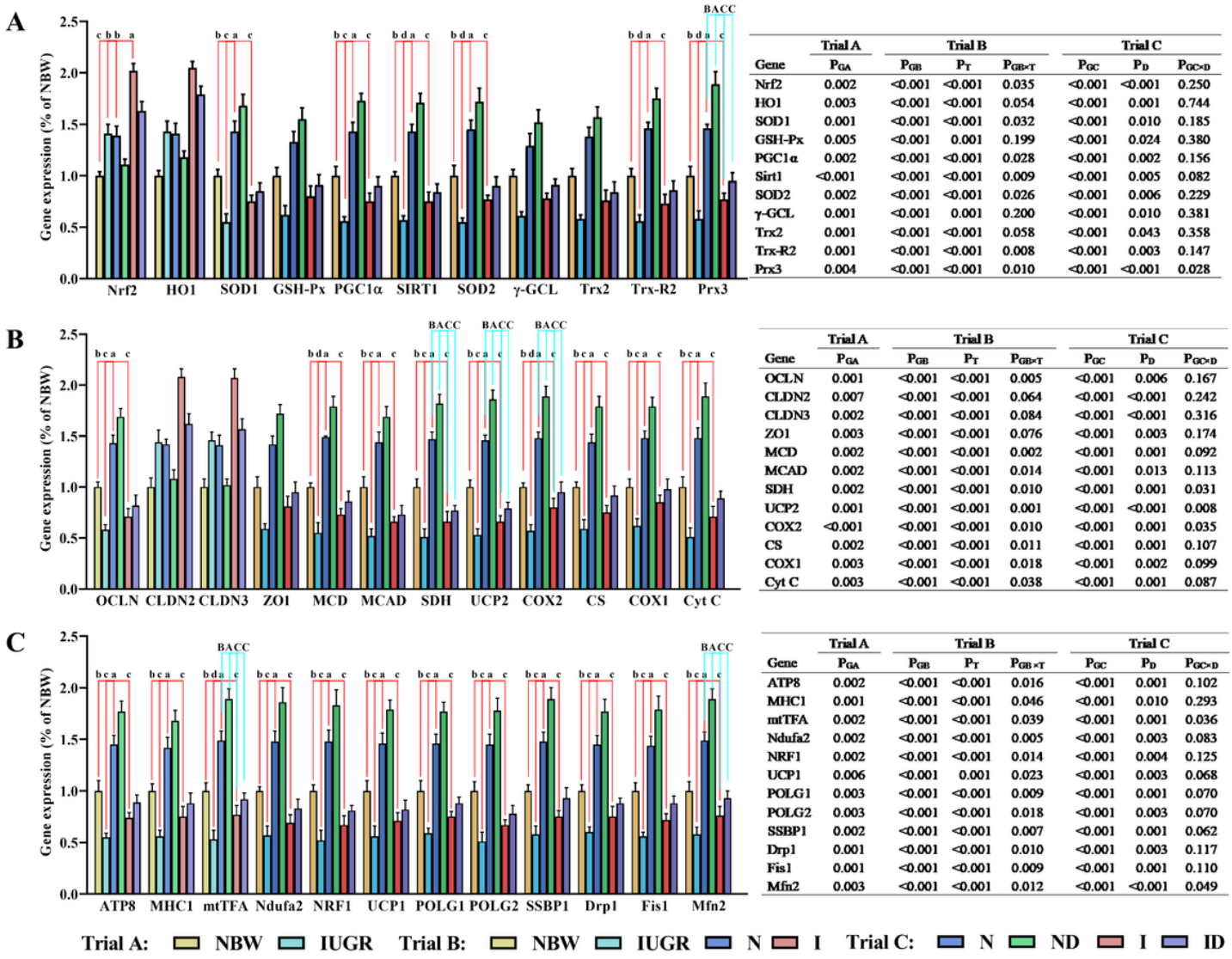

Gene	Trial A	Trial B			Trial C		
	P_{GA}	P_{GB}	P_{T}	$P_{GB\times T}$	P_{GC}	P_{D}	$P_{GC\times D}$
Nrf2	0.002	<0.001	<0.001	0.035	<0.001	<0.001	0.250
HO1	0.003	<0.001	<0.001	0.054	<0.001	0.001	0.744
SOD1	0.001	<0.001	<0.001	0.032	<0.001	0.010	0.185
GSH-Px	0.005	<0.001	0.001	0.199	<0.001	0.024	0.380
PGC1α	0.002	<0.001	<0.001	0.028	<0.001	0.002	0.156
Sirt1	<0.001	<0.001	<0.001	0.009	<0.001	0.005	0.082
SOD2	0.002	<0.001	<0.001	0.026	<0.001	0.006	0.229
γ-GCL	0.001	<0.001	0.001	0.200	<0.001	0.010	0.381
Trx2	0.001	<0.001	<0.001	0.058	<0.001	0.043	0.358
Trx-R2	0.001	<0.001	<0.001	0.008	<0.001	0.003	0.147
Prx3	0.004	<0.001	<0.001	0.010	<0.001	<0.001	0.028

Gene	Trial A	Trial B			Trial C		
	P_{GA}	P_{GB}	P_{T}	$P_{GB\times T}$	P_{GC}	P_{D}	$P_{GC\times D}$
OCLN	0.001	<0.001	<0.001	0.005	<0.001	0.006	0.167
CLDN2	0.007	<0.001	<0.001	0.064	<0.001	<0.001	0.242
CLDN3	0.002	<0.001	<0.001	0.084	<0.001	<0.001	0.316
ZO1	0.003	<0.001	<0.001	0.076	<0.001	0.003	0.174
MCD	0.002	<0.001	<0.001	0.002	<0.001	0.001	0.092
MCAD	0.002	<0.001	<0.001	0.014	<0.001	0.013	0.113
SDH	0.002	<0.001	<0.001	0.010	<0.001	0.001	0.031
UCP2	0.001	<0.001	<0.001	0.001	<0.001	<0.001	0.008
COX2	<0.001	<0.001	<0.001	0.010	<0.001	0.001	0.035
CS	0.002	<0.001	<0.001	0.011	<0.001	0.001	0.107
COX1	0.003	<0.001	<0.001	0.018	<0.001	0.002	0.099
Cyt C	0.003	<0.001	<0.001	0.038	<0.001	0.001	0.087

Gene	Trial A	Trial B			Trial C		
	P_{GA}	P_{GB}	P_{T}	$P_{GB\times T}$	P_{GC}	P_{D}	$P_{GC\times D}$
ATP8	0.002	<0.001	<0.001	0.016	<0.001	0.001	0.102
MHC1	0.001	<0.001	<0.001	0.046	<0.001	0.010	0.293
mtTFA	0.002	<0.001	<0.001	0.039	<0.001	0.001	0.036
Ndufa2	0.002	<0.001	<0.001	0.005	<0.001	0.003	0.083
NRF1	0.002	<0.001	<0.001	0.014	<0.001	0.004	0.125
UCP1	0.006	<0.001	0.001	0.023	<0.001	0.003	0.068
POLG1	0.003	<0.001	<0.001	0.009	<0.001	0.001	0.070
POLG2	0.003	<0.001	<0.001	0.018	<0.001	0.003	0.070
SSBP1	0.002	<0.001	<0.001	0.007	<0.001	0.001	0.062
Drp1	0.001	<0.001	<0.001	0.010	<0.001	0.003	0.117
Fis1	0.001	<0.001	<0.001	0.009	<0.001	0.001	0.110
Mfn2	0.003	<0.001	<0.001	0.012	<0.001	<0.001	0.049

Figure 8

Dietary DMG-Na supplementation improved the jejunum gene expression of IUGR piglets during the suckling period. Data are expressed as the mean ± SD, n = 10. Different superscripts * (Trial A: NBW, IUGR group in black color), and a, b, c, d (Trial B: NBW, IUGR, N, I group in red color), and A, B, C, D (Trial C: N, ND, I, ID group in blue color) represent significant differences ($P < 0.05$). NBW represents normal birth weight newborn piglets; IUGR represents intrauterine growth restriction newborn piglets; N represents NBW piglets fed a basic milk diet; ND represents NBW piglets fed a basic milk diet supplemented with 0.1% DMG-Na; I represents IUGR piglets fed a basic milk diet; ID represents IUGR piglets fed a basic milk diet supplemented with 0.1% DMG-Na. Nrf2, nuclear factor erythroid 2-related factor 2; HO1, heme oxygenase 1; SOD1, copper and zinc superoxide dismutase; GSH-Px, glutathione peroxidase; Sirt1, sirtuin 1; PGC1α, peroxisome proliferator-activated receptorγcoactivator-1α; SOD2, manganese superoxide dismutase; γ-GCL, γ-glutamylcysteine ligase; Trx2, thioredoxin 2; Trx-R2, thioredoxin reductase 2; Prx3, peroxiredoxin 3; OCLN, occluding; CLDN2, cloudin2; CLDN3, cloudin3; ZO1, zonula occludens-1; MCD, lipid oxidation enzymes malonyl-CoA decarboxylase; MCAD, medium-chain acyl-CoA dehydrogenase; SDH,

mitochondrial proteins succinate dehydrogenase; UCP2, uncoupling protein 2; COX2, cyclooxygenase 2; CS, citrate synthase; COX1, cyclooxygenase 1; Cyt C, Cytochrome C; ATP8, mitochondrially encoded ATP synthase membrane subunit 8; MHC1, major histocompatibility complex I; mtTFA, mitochondrial transcription factor A; Ndufa2, NADH dehydrogenase (ubiquinone) iron-sulfur protein 2; NRF1, nuclear respiratory factor 1; UCP1, uncoupling protein 1; POLG1, γ DNA polymerases catalytic subunit; POLG2, γ DNA polymerases accessory subunit; SSBP1, single-strand DNA binding protein 1; Drp1, dynamin-related protein 1; Fis1, mitochondrial fission 1; Mfn2, mitochondrial mitofusin2.

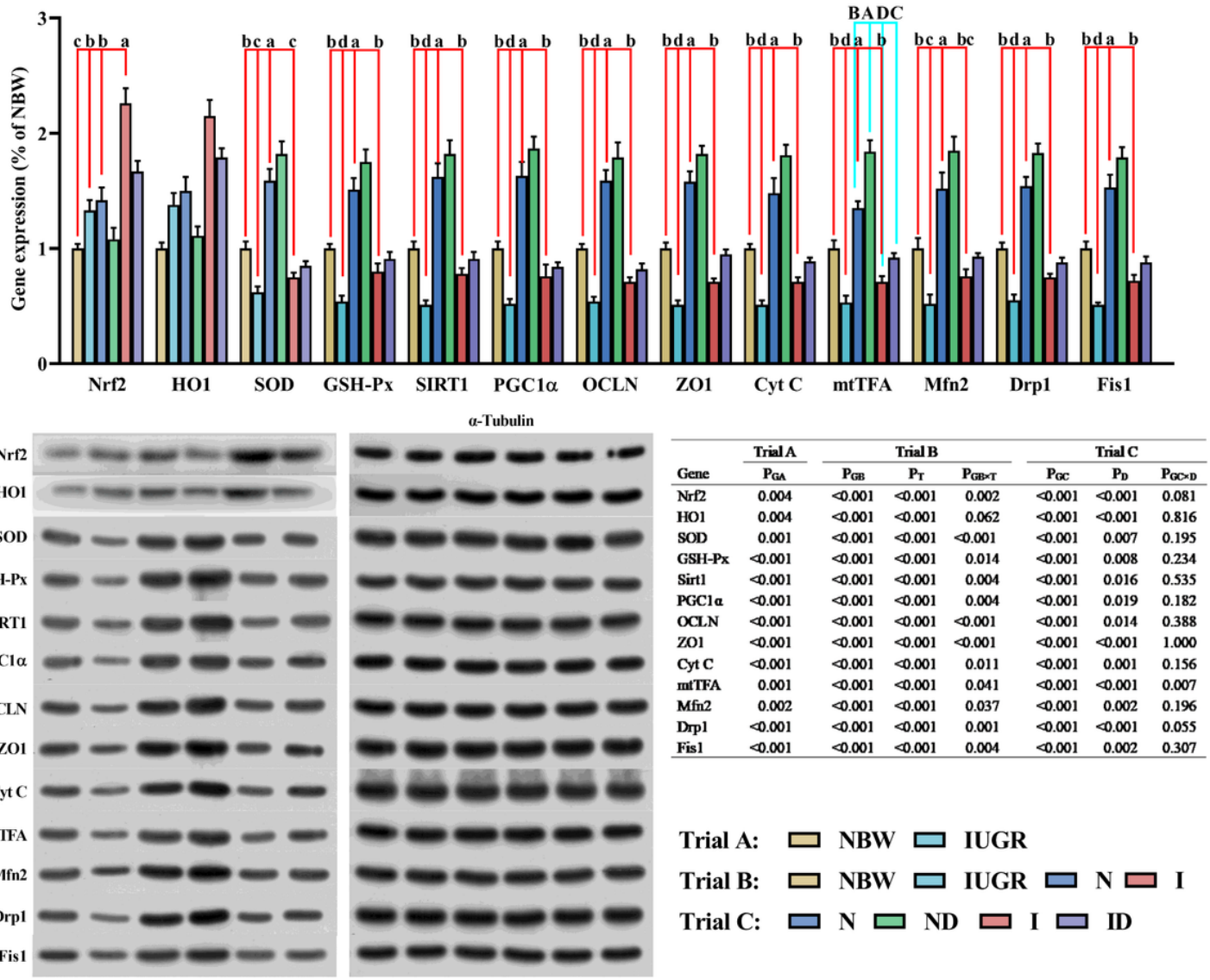

Gene	Trial A	Trial B			Trial C		
	P_{GA}	P_{GB}	P_T	$P_{GB\times T}$	P_{GC}	P_D	$P_{GC\times D}$
Nrf2	0.004	<0.001	<0.001	0.002	<0.001	<0.001	0.081
HO1	0.004	<0.001	<0.001	0.062	<0.001	<0.001	0.816
SOD	0.001	<0.001	<0.001	<0.001	<0.001	0.007	0.195
GSH-Px	<0.001	<0.001	<0.001	0.014	<0.001	0.008	0.234
Sirt1	<0.001	<0.001	<0.001	0.004	<0.001	0.016	0.535
PGC1α	<0.001	<0.001	<0.001	0.004	<0.001	0.019	0.182
OCLN	<0.001	<0.001	<0.001	<0.001	<0.001	0.014	0.388
ZO1	<0.001	<0.001	<0.001	<0.001	<0.001	<0.001	1.000
Cyt C	<0.001	<0.001	<0.001	0.011	<0.001	0.001	0.156
mtTFA	0.001	<0.001	<0.001	0.041	<0.001	<0.001	0.007
Mfn2	0.002	<0.001	<0.001	0.037	<0.001	0.002	0.196
Drp1	<0.001	<0.001	<0.001	0.001	<0.001	<0.001	0.055
Fis1	<0.001	<0.001	<0.001	0.004	<0.001	0.002	0.307

Figure 9

Dietary DMG-Na supplementation improved the jejunum protein expression of IUGR piglets during the suckling period. Data are expressed as the mean ± SD, n = 10. Different superscripts * (Trial A: NBW, IUGR group in black color), and a, b, c, d (Trial B: NBW, IUGR, N, I group in red color), and A, B, C, D (Trial C: N, ND, I, ID group in blue color) represent significant differences ($P < 0.05$). NBW represents normal birth weight newborn piglets; IUGR represents intrauterine growth restriction newborn piglets; N represents

NBW piglets fed a basic milk diet; ND represents NBW piglets fed a basic milk diet supplemented with 0.1% DMG-Na; I represents IUGR piglets fed a basic milk diet; ID represents IUGR piglets fed a basic milk diet supplemented with 0.1% DMG-Na. Nrf2, nuclear factor erythroid 2-related factor 2; HO1, heme oxygenase 1; SOD, superoxide dismutase; GSH-Px, glutathione peroxidase; Sirt1, sirtuin 1; PGC1α, peroxisome proliferator-activated receptorγcoactivator-1α; OCLN, occluding; ZO1, zonula occludens-1; Cyt C, Cytochrome C; mtTFA, mitochondrial transcription factor A; Mfn2, mitochondrial mitofusin2; Drp1, dynamin-related protein 1; Fis1, mitochondrial fission 1.

Supplementary Files

This is a list of supplementary files associated with this preprint. Click to download.

- Supplementaryinformation.docx